Plant, Cell & Environment

WILEY

Plant, Cell & Environment

ORIGINAL ARTICLE

VaEIN3.1-VaERF057-VaFBA1 Module Positively Regulates Cold Tolerance by Accumulating Soluble Sugar in Grapevine

Huimin Zhou[1,2] | Yujun Hou[1,2] | Lisha Tan[1] | Qingyun Li[1,2] | Wenjuan Li[1,2] | Subash Kafle[1,2] | Meilong Xu[3] | Konstantin V. Kiselev[4] | Lin Meng[1] | Haiping Xin[1]

[1]State Key Laboratory of Plant Diversity and Specialty Crops, Wuhan Botanical Garden, Chinese Academy of Sciences, Wuhan, China | [2]University of Chinese Academy of Sciences, Beijing, China | [3]Institute of Horticulture, Ningxia Academy of Agriculture and Forestry Science, Yinchuan, China | [4]Laboratory of Biotechnology, Federal Scientific Center of the East Asia Terrestrial Biodiversity FEB RAS, Vladivostok, Russia

Correspondence: Haiping Xin (xinhaiping@wbgcas.cn)

Received: 13 December 2024 | **Accepted:** 20 March 2025

Funding: This work was supported by the Grape Breeding Project of Ningxia (NXNYYZ202101-04), the Natural Science Foundation of China (32302517) and the Project funded by the China Postdoctoral Science Foundation (2023M733717).

Keywords: cold stress | grapevine | soluble sugar | *VaERF057* | *VaFBA1*

ABSTRACT

Ethylene-responsive transcription factors (ERFs) were widely found to participate in cold response in plants. But the underlying regulatory mechanism of each cold-induced ERFs remains to be elucidated. Previously, we identified *VaERF057* as a cold-induced gene in *Vitis amurensis*, a cold-hardy wild *Vitis* species. Here we found that overexpression of *VaERF057* (*VaERF057*-OE) enhanced the freezing tolerance of *V. amurensis* roots. While *VaERF057* knockdown tissues show decreased cold tolerance than control. DAP-seq combined with transcriptome data (*VaERF057*-OE roots) allowed to identify *VaFBA1* (fructose-1,6-bisphosphate aldolase) as a downstream target of VaERF057. VaERF057 can bind to the *VaFBA1* promoters and activate its expression. *VaERF057*-OE roots show increased expression of *VaFBA1* and high content of soluble sugar than the control, whereas *VaERF057* knockdown tissues showed opposite changes. Results from OE and knockdown material also support the role of *VaFBA1* in regulating soluble sugar content and cold tolerance in grapevines. Furthermore, cold-induced expression of *VaERF057* was found to be regulated by ethylene-insensitive3-1 (*VaEIN3.1*). Overexpression of *VaEIN3.1* enhanced the transcription of *VaERF057* and *VaFBA1*, the content of soluble sugar and cold tolerance in grapevine. *VaEIN3.1* knockdown tissues show opposite trends when compared to *VaEIN3.1*-OE lines. Together, these results suggested a positive contribution of VaEIN3.1-VaERF057-VaFBA1 module in response to cold stress in grapevine.

1 | Introduction

Grapevine is an economically valuable fruit crop that is widely cultivated around the world. Cold stress such as late frost in spring and extremely low temperature below −15°C in winter can damage the germinated tissues or dormant branches and buds of grapevine (Fennell 2004; Xin et al. 2013). In the past decade, lots of works focused on transcriptional, translational and metabolic modification of grapevines under low temperature, and the functions of several transcription factors (TFs) were also discovered (Ren et al. 2023; Q. Li et al. 2025; Hou et al. 2024). These studies focused not only on cold-sensitive species *Vitis vinifera* but also on wild cold-tolerant species *Vitis amurensis* whose branches and vines are capable of surviving in extremely low temperatures of −40°C (Fennell 2004). Uncovering the regulatory mechanism of how the grapevine

responds to cold stress and identifying the key pathways and genes that positively contributed to this process may finally shed light on breeding new grapevine cultivars with excellent cold tolerance.

The APETALA2/ethylene-responsive element-binding factor (AP2/ERF) represents a group of the plant-specific TFs and was classified into four subfamilies, ERF, AP2, DREB (dehydration responsive element-binding protein) and RAV (related to ABI3/VP1) based on the presence of one or two AP2 structural domains with DNA-binding functions (Sakuma et al. 2002). AP2/ERF TFs were found to participate in multiple developmental and stress response processes in plants by specifically binding to GCC-box or DREB repeat sequences located within the promoter regions of downstream genes (Yamaguchi-Shinozaki and Shinozaki 1994; Ohme-Takagi and Shinshi 1995). ERF subfamily comprises the most extensive group in the AP2/ERF superfamily, and its biological function has been widely studied (Wu et al. 2022). The members of the ERF subfamily respond to abiotic stresses including cold, drought and salinity in plants (Yao et al. 2017; Dubouzet et al. 2003; Zhuo et al. 2018). A considerable number of *ERFs* were reported to function during low-temperature conditions and contributed to the cold hardiness of plants (Huang et al. 2023). Overexpression (OE) of *PtrERF109*, *PtrERF108*, and *PtrERF110* increased the cold tolerance of trifoliate orange by regulating the expression of the peroxidase gene (*PtrPrx1*), the raffinose synthase gene (*PtrRafS*) and the sucrose phosphate synthase 4 gene (*PtrSPS4*), respectively (M. Wang et al. 2019; Khan et al. 2021, 2024). OE *BpERF13* enhances freezing tolerance in birch by regulating the expression of *CBF* genes and mitigating reactive oxygen species (ROS) accumulation (Lv et al. 2020). In grapevine, *VaERF092* interacts with the GCC-box in *VaWRKY33* promoter, thereby activating its expression to improve cold tolerance (X. Sun et al. 2019). These results indicate the functional differentiation of *ERFs* during stress response in plants.

Sugars serve not only as a fundamental energy source essential for maintaining normal plant growth and development but also as a critical component in plant cells (O'Hara et al. 2013). Moreover, increased evidence indicates that sugars play crucial roles in plant stress response. Soluble sugars function as osmoprotectants to stabilise osmotic balance and also contribute to scavenging of ROS scavenging (Contento et al. 2004; Couée et al. 2006; Sperdouli and Moustakas 2012). Fructose-1,6-bisphosphate aldolases (FBAs) are pivotal glycolytic enzymes that catalyse the reversible cleavage of fructose-1,6-bisphosphate into dihydroxyacetone phosphate and glyceraldehyde 3-phosphate to facilitate in breakdown of sugars and provide carbon skeletons and ATP for anabolic processes (Rutter 1964; Plaxton 1996). In *Arabidopsis thaliana*, a total of eight FBA genes were identified, and its responses to abnormal temperature were reported (Lu et al. 2012). The silence of *SlFBA7* in *Solanum lycopersicum* was observed to result in decreasing FBA activity and soluble sugar content (Cai et al. 2018). OE of *TaFBA-A10* enhanced freezing tolerance of transgenic *Arabidopsis* by regulating Calvin cycle and glycolysis rate (Peng et al. 2022). The activity of FBA in alfalfa was observed to increase following low-temperature treatment, and CML10 interacts with FBA6 to enhance the accumulation of soluble sugars and positively regulate cold tolerance (S. Yu et al. 2022). These results highlighted the roles of *FBAs* during cold stress response in plants, but the transcriptional regulation of *FBAs* is still unknown and needs to be elucidated.

Ethylene synthesis is induced under cold stress in many plants such as apple and grapevine (X. Sun et al. 2016; Y. Wang et al. 2021). The ethylene signalling cascade begins from the sense of the perception of the ethylene by the receptors (Alonso and Stepanova 2004; Zhao et al. 2021). The interaction between ethylene and receptors suppresses the downstream kinase constitutive triple response 1 (CTR1) and activates ethylene-insensitive 2 (EIN2) in the cytoplasm. Subsequently, the carboxyl end of EIN2 (EIN2 CEND) is transferred into the nucleus and promoted the accumulation of TF ethylene-insensitive 3 (EIN3) and its homologue EIN3-LIKE 1 (EIL1). EIN3/EIL1 regulates the expression of downstream ethylene-responsive genes by specifically binding to the EBS (EIN3-binding site) cis-elements located in their promoter regions (Zhao et al. 2021). In *Arabidopsis*, one EIN3, along with five related EIN3-like genes, has been identified (Chao et al. 1997). AtEIN3 was found to inhibit the expression of cold-responsive genes such as *AtCBFs*, *AtARR7* and *AtARR15*, thereby reducing freezing tolerance (Shi et al. 2012). While in tomato, *SlEIL2* and *SlEIL7* were found to protect photosystem II (PSII) under low temperature (M. Zhang et al. 2023). Ethylene signalling regulates hundreds of genes during cold stress in grapevines (Hou et al. 2023). But how the *EIN3/EIL* members regulate these ethylene-responsive genes remains to be discovered.

Previously, we showed that low temperature could promote ethylene release in grapevine and induce the expression of *ERF057* in the leaves of *V. amurensis* and *V. vinifera* cv. 'Muscat Hamburg' (X. Sun et al. 2016). *VaERF057* exhibits binding activation to both GCC-box and DRE elements, and its OE line of *Arabidopsis* shows improved cold tolerance (X. Sun et al. 2016). In this study, the signalling pathways regulated by *VaERF057* were studied. *Agrobacterium rhizogenes*-induced hairy root transformation system and virus-induced gene silencing (VIGS) in leaves were employed to generate OE and knockdown materials for target genes. The downstream gene of *VaERF057* was identified, and transcriptional regulation was validated by yeast one-hybrid (YIH), dual-luciferase (LUC) assay and electromobility shift assay (EMSA). The role of *VaFBA1* in enhancing soluble sugar content and conferring cold tolerance in grapevine was checked in OE and mutagenised root lines, as well as knockdown lines by VIGS in the leaves of grapevines. Additionally, the *VaEIN3.1* as an upstream regulation factor of *VaERF057* was investigated through a series of experiments. The findings not only uncover the role of VaEIN3.1-VaERF057-VaFBA1 module in responding to cold stress in grapevine but also provide new clues for ethylene regulatory network under cold stress in plants.

2 | Experimental Procedures

2.1 | Plant Materials and Growth Conditions

The plantlets of *V. amurensis* were cultivated on half-strength Murashige and Skoog (1/2 MS) medium containing 0.58 g/L MES, 30 g/L sucrose, 7 g/L agar, with the pH adjusted to 5.8.

The plantlets were kept at 26°C under a 16 h light/8 h dark photoperiod with a light intensity 100 μmol m^{-2} s^{-1}. After 6 weeks, the seedlings were transferred to a growth chamber where the temperature was set to 4°C. The third fully developed leaves were collected at 0, 2, 4, 8, 24 and 48 h and frozen in liquid nitrogen and stored at −80°C for subsequent analysis.

2.2 | RNA Extraction and Quantitative Real-Time-Polymerase Chain Reaction Analysis

Total RNA was isolated from collected samples by using RNAprep pure plant plus kit (TIANGEN, Beijing, China) in accordance with the manufacturer's protocol. cDNA was generated via HiScript III 1st Strand cDNA Synthesis Kit with gDNA wiper (Vazyme, Nanjing, China). Quantitative real-time (qRT)-polymerase chain reaction (PCR) was performed on the QuantStudio 6 Flex PCR system (Applied Biosystems, USA) with TransStart Top Green qPCR SuperMix (TransGen, Beijing, China). Each 20 μL of reaction mixture contained 10 μL of 2× TransStart Top Green qPCR SuperMix, 100 ng of cDNA and 0.2 μM of forward and reverse primers. Relative expression levels of each gene were quantified by the $2^{-\Delta\Delta CT}$ method. The experiment was conducted with three independent biological replicates. The primer sequences are shown in Supporting Information S2: Table 1.

2.3 | Gene Cloning and Sequence Analysis

The full-length ORF of *VaERF057*, *VaFBA1* and *VaEIN3.1* were amplified via PCR using *V. amurensis* leaf cDNA as template with designated primer (Supporting Information S2: Table 1). The phylogenetic tree of the ERF family was constructed using a total of 122 ERF protein sequences, including 121 from *Arabidopsis*, 1 from grapevine. The phylogenetic tree of the FBA family was constructed using a total of nine FBA protein sequences, including eight from *Arabidopsis*, one from grapevine. The phylogenetic tree of the EIN3/EIL family was constructed using a total of nine EIN3/EIL protein sequences, including five from *Arabidopsis*, four from grapevine. The neighbour-joining method in MEGA11 (Tamura et al. 2021) was used to construct the trees.

2.4 | Analysis of *VaERF057* Promoter Activity

A 2000-bp promoter fragment of *VaERF057* (upstream of ATG) was amplified and inserted into the pBI101-GUS vector. The resulting recombinant plasmid p*VaERF057*: GUS was introduced into *Agrobacterium tumefaciens* strain GV3101. Subsequently, *Agrobacterium* harbouring either recombinant or empty vector (EV) was inoculated into *Nicotiana benthamiana* leaves following the method outlined by X. Sun et al. (2019). Postinoculation, the plants were cultivated under the dark for 2 days, followed by low-temperature treatment at 8°C for 2 h. GUS activity was assessed using the histochemical assay kit (Zhongkeruitei, China), and the staining intensity was quantified using the ImageJ software.

2.5 | Subcellular Location Analysis

The ORF of *VaERF057* (without the stop codon) was in-frame linked with the green fluorescent protein (GFP) gene in the pSAK277-eGFP vector. The resultant recombinant vector 35S: VaERF057-GFP and EV 35S: GFP were introduced into *A. tumefaciens* strain GV3101, respectively. After cultivation, the *Agrobacterium* was mixed with GV3101 carrying the VirD2NLS mCherry (nucleus marker) and co-introduced into *N. benthamiana* leaves according to the protocol described by Geng and Liu (2018). A Leica TCS SP8 confocal laser-scanning microscope was used to capture the fluorescence signals from GFP and red fluorescent protein (RFP).

2.6 | Transcriptional Activation Activity Assay

The full-length and truncated fragments (1–132 aa, 133–316 aa) of VaERF057 were constructed into the pGBKT7 vector. The pGBKT7-p53 was used as a positive control, and pGBKT7 served as a negative control. All plasmids were introduced into the yeast strain AH109. The transcriptional activation activity of the transformed yeast cells was evaluated via plating the transformants on selective medium including SD/-Trp, SD/-Trp/-His/-Ade and SD/-Trp/-His/-Ade/X-α-gal at 30°C for 3 days.

2.7 | Genetic Transformation and Identification of Positive Materials

The codon regions of target genes were amplified and ligated into pSAK277 to generate pSAK277-VaERF057, pSAK277-VaFBA1 and pSAK277-VaEIN3.1-OE vectors, and pSAK277 was used as a control. To create loss-of-function lines, CRISPR/Cas9 was used to edit *VaERF057* and *VaFBA1*. The specific target sequence was predicted using the CRISPR-P online tool (http://crispr.hzau.edu.cn/cgi-bin/CRISPR2/SCORE) and incorporated into single-guide RNA (sgRNA). The sgRNA expression cassette containing two target sequences (DT1 and DT2) was amplified via PCR using pCBC-DT1T2 as template, followed by purification with the TIANgel midi purification kit (TIANGEN, Beijing, China). Both the purified PCR products and pKSE401 were digested with *Bsa*I and ligated with T4 DNA ligase. Positive clones were screened, and the plasmid was isolated and transformed into *A. rhizogenes* MSU440. The primers are provided in Supporting Information S2: Table 1.

Grapevine hairy root transformation was performed following the method described by Hou et al. (2024). *Agrobacterium* was cultured overnight in liquid TY medium supplemented with different antibiotics (streptomycin for MSU440, spectinomycin for pSAK277 and kanamycin for pKSE401) until OD_{600} reached 0.8. Then, *Agrobacterium* was collected, and the OD_{600} was adjusted to 0.4 by fresh medium with 100 μM acetosyringone (AS) and incubated at 28°C for 2–3 h. The stems of grapevine (*V. amurensis*) seedlings were cut into 2 cm and then immersed in the activated *Agrobacterium* solution for 8 min. After immersion, stems were cultured on 1/2 MS medium and kept in darkness at 25°C for 2 days. Then, stems were rinsed three

times with distilled water containing 400 mg/L ceftazidime (Cef) and 400 mg/L carbenicillin (Carb). Then, stems were cultivated in 1/2 MS solid medium containing 15 mg/L kanamycin, 200 mg/L Cef and 200 mg/L Carb. After 4 weeks, genomic PCR and qRT-PCR analyses were utilised to identify positive transgenic lines. CRISPR/Cas9-edited plants were further analysed using the Hi-TOM (high-throughput tracking or mutations) platform to assess the mutation efficiency (Q. Liu et al. 2019).

As for the hairy root transformation system used here, each root is considered as a single line since the roots germinated from the different positions of the explants after agrobacterium infection. When electrolyte leakage (EL) was detected, a single root was used as one biological replicate, and more than five roots were used to calculate the EL for OE or KO materials. For MDA and soluble sugar contents, the biomass of a single root is not enough for detection. Thus, three roots were pooled together and considered as a single biological replicate, and three independent replicates were analysed in total.

For VIGS, a non-conserved fragment of *VaERF057*, *VaFBA1* and *VaEIN3.1* (shown in Supporting Information S2: Table 2) was inserted into the pTRV2 vector. The resulting pTRV1, pTRV2, pTRV2-VaERF057, pTRV2-VaFBA1 and pTRV2-VaEIN3.1 vectors were individually introduced into *A. tumefaciens* strain GV3101, respectively. The pTRV1 bacterial suspension was mixed with either pTRV2-VaERF057/pTRV2-VaFBA1/pTRV2-VaEIN3.1 or pTRV2 and then infiltrated into 6-week-old *V. amurensis* plantlets following the previously described method (Mu et al. 2023). In brief, the plantlets were subjected to vacuum infiltration at −90 kPa for 20 min. After infiltration, the plantlets were washed with distilled water, transplanted into solid growth medium (peat soil:vermiculite = 1:1) and kept in the dark for the first 3 days. Each treatment included three biological replicates, with three plantlets per replicate. The transcriptional levels of target genes in transformed plants were checked by qRT-PCR.

2.8 | Cold Tolerance Assays

As for cold acclimation (CA), 4°C was used to induce a range of physiological and biochemical changes in plant materials without leading to lethality. The 8-h duration of CA was selected because of considerable transcription level of *VaERF057* was induced at that time. Therefore, soluble sugar, malondialdehyde (MDA), $O_2^{\cdot-}$ and H_2O_2 content were measured in transgenic grapevine roots at 25°C or 4°C for 8 h, respectively.

To evaluate the cold tolerance of roots that transformed with EV, OE and knock-out (KO) vectors, the EL of EV roots at −1°C, −2°C, −3°C, −4°C, −5°C, −6°C and −7°C for 4 h were checked. The EL of EV roots was about 50%–70% under −5°C for 4 h (Supporting Information S2: Table 3). Thus, the OE and KO roots were treated at −5°C for 4 h to compare the cold tolerance with EV roots. Four-week-old roots were treated at 25°C or −5°C for 4 h and incubated at 4°C for 12 h in the dark and then for EL measurement.

For VIGS plants, the leaves of seedling show loss of turgor pressure and wilting phenotype when treated at −5°C for 5 h and recovered later. Thus, 2 weeks after infiltration, the VIGS seedlings were subjected to −5°C for 5 h and samples were obtained for physiological and gene expression analysis.

2.9 | Physiological Measurement

EL was quantified based on previous report (Amor et al. 2007). In brief, the samples were cut and submerged in 5 mL of double-distilled water (ddH_2O), followed by shaking at 40 rpm for 2 h. A conductivity meter (FiveEasy Plus FE38, Mettler-Toledo, Switzerland) was used to record the initial conductivity values (E1) of each sample and the ddH_2O control (C1). A water bath was utilised to maintain all samples at 100°C for 1 h, followed by cooling to room temperature after which the final conductivity values (E2, C2) were recorded. The EL ratio was determined using the following formula: $EL = (E1 - C1)/(E2 - C2) \times 100\%$. The commercial assay kits (A003-1 for MDA, A064-1 for H_2O_2, A052-1 for $O_2^{\cdot-}$, Nanjing Jiancheng Bioengineering Institute, China) were used to quantify the MDA content, H_2O_2 content and $O_2^{\cdot-}$ level following the manufacturer's protocols. The contents of sugar were analysed using the method described by Zhou et al. (2023). For histochemical staining, 3,3-diaminobenzidine (DAB) and nitro blue tetrazolium (NBT) were employed to perform H_2O_2 and $O_2^{\cdot-}$ staining, respectively (Khan et al. 2024).

2.10 | RNA-Sequencing Analysis

Total RNAs were extracted from the EV and OE-VaERF057 roots by RNAprep Pure Plant Kit (Tiangen, Beijing, China). Three replicates were conducted for each sample. The integrity and the quantity of the RNAs were evaluated using a NanoDrop ND 2000 spectrophotometer (Thermo Fisher Scientific, Waltham, MA, USA), which were further verified by 1.2% agarose gel electrophoresis. Following the removal of low-quality reads, high-quality reads were aligned to the *V. vinifera* cv. 'Pinot Noir' reference genome which is available on the phytozome database (https://phytozome-next.jgi.doe.gov/info/Vvinifera_v2_1) using HISAT and Bowtie2. The expression levels of each gene were estimated by fragments per kilobase of exon model per million mapped fragments (FPKM) values. Genes exhibiting a fold change ≥ 2 and an adjusted *p*-value (FDR) < 0.05 were classified as differentially expressed genes (DEGs). The KEGG enrichment analysis, implemented in the TBtools, was utilised to perform pathway enrichment analysis of DEGs (C. Chen et al. 2023).

2.11 | DNA Affinity Purification Sequencing Assay

The DNA affinity purification sequencing (DAP-seq) assay was conducted by Bluescape (Baoding, China) to identify genome-wide protein–DNA interactions as mentioned by Bartlett et al. (2017). Cetyltrimethylammonium bromide (CTAB) was used to isolate genomic DNA from the leaves of *V. amurensis*.

The extracted genomic DNA was sheared to 200-bp fragment using a Covaris M220 (Woburn, MA, USA) in accordance with the manufacturer's guidelines. After fragmentation, the genomic DNA was purified by MICH DNA Clean Beads (NGS-0201-100, Bluescape Hebei Biotech, Baoding, China) with two independent biological replicates. Library construction was performed by the MICH TLX DNA-Seq Kit (NGS 0602-24, Bluescape Hebei Biotech, Baoding, China). The CDS of *VaERF057* was inserted into pFN19K (HaloTag) T7 SP6 Flexi vector. Expressed Halo-VaERF057 proteins were specifically bound and isolated through Magne Halo Tag Beads (Promega), followed by incubation with the constructed DNA library. And then the VaERF057-binding DNA fragments were eluted and sequenced via an Illumina NovaSeq. Input libraries, generated in the absence of the addition of VaERF057 protein, served as negative controls. Clean reads were derived from raw data by applying the fastp software with default parameters for downstream analysis.

The high-quality clean reads were mapped to the published genome of *V. vinifera* cv. 'Pinot Noir', which is available on the phytozome database using BWA-MEM (Burrows-wheeler aligner-maximum matching). And then filtered for reads with a mapping quality score (MAPQ) > 30 was retained using SAMtools. Peaks were identified using MACS (model-based analysis of ChIP-Seq) to discover the binding sites (Y. Zhang et al. 2008). Furthermore, the peaks from the two biological replicates with p-value < 0.05 were merged using IDR (irreproducibility discovery rate). The MEME-ChIP software was employed to identify conserved motifs within the peak region (Machanick and Bailey 2011). Peaks annotation was performed using ChIPseeker software (G. Yu et al. 2015).

2.12 | YIH Screening and Assays

The interaction of VaERF057 with *VaFBA1* promoter, as well as the binding of *VaEIN3.1* to *VaERF057* promoter, was investigated using YIH assay. The full-length CDS of *VaERF057* and *VaEIN3.1* was inserted into the *Eco*RI and *Bam*HI sites of the pGADT7 vector to create prey vectors. For the bait constructs, promoter fragments of *VaFBA1* containing GCCCAC motif were cloned into the pAbAi vector, while mutated bait with the GCCCAC replaced by AAAAAA was also constructed. Similarly, promoter fragments of *VaERF057* containing ATGTA motif were cloned into the pAbAi vector, and mutated bait with the ATGTA replaced by CCCCC was generated. Y1H assay was constructed by the Matchmaker Y1H Library Screening System (Clontech, USA). Coexpressed yeast cells harbouring the prey vector and different bait vectors were cultured on SD/-Leu/-Ura medium or SD/-Leu/-Ura + AbA (Aureobasidin) and incubated for 3 days. The pGADT7-AD + bait served as the negative control, and pAbAi-p53 + pGADT7-p53 served as positive controls.

2.13 | Dual-LUC Assay

To generate an effector, the full-length CDS of *VaERF057* was cloned into the pGreenII 62-SK vector. The reporters were generated by cloning the wild-type and mutagenised promoter sequences of *VaFBA1* into pGreenII 0800-LUC vector to generate reporters. Using *A. tumefaciens*-mediated infiltration, the effector and reporter vectors were transiently coexpressed in *N. benthamiana* leaves. The quantification of LUC activities was performed with the Dual-Luciferase Reporter Assay System (Promega, USA). Briefly, the infiltrated leaves were treated with D-Luciferin solution (1 mM) and kept in darkness for 5 min to ensure the absorption of substrate. Then, the LUC fluorescence signals were captured using a cooled CCD camera integrated into a plant living imaging system (ChemiScope 6000, China).

2.14 | Electrophoretic Mobility Shift Assay

The full-length *VaERF057* and *VaEIN3.1* were inserted into the pET-28a expression vector, which contains 6× His tag, and the resultant recombinant vector was introduced into *Escherichia coli* strain Rosetta (DE3). The His-tagged fused protein (His-VaERF057 or His-VaEIN3.1) was induced by 0.5 mM isopropyl-β-D-1-thiogalactopyranoside (IPTG) at 30°C for 6 h. Using the Qiagen Ni-NTA Agarose kit, protein purification was carried out. The probes, containing either wild-type elements or mutated elements, were synthesised with 5-carboxyfluorescein (5′-FAM) labelling by Tsingke Biological Technology (Beijing, China). The LightShift Chemiluminescent EMSA Kit (Thermo) was used to perform the EMSA. Separation of the reaction mixtures was achieved on 6.5% non-denaturing polyacrylamide gel in 0.5× TBE running buffer. The fluorescence signals were detected and analysed using the Typhoon FLA9500 scanner (GE Healthcare, Vienna, Austria).

2.15 | Statistical Analysis

All experiments were replicated three times. All data were presented as the mean ± standard error (SE). Statistical analyses were conducted by means of one-way analysis of variance (ANOVA) with Duncan's multiple range test in GraphPad prism (version 8.3.0). Significance levels were defined as $p < 0.05$ (*) and $p < 0.01$ (**). Different letters (e.g., a–c) indicate significant differences ($p < 0.05$).

3 | Results

3.1 | VaERF057 Is Localised in the Nucleus With Transcriptional Activation Activity

The expression patterns of *VaERF057* in grapevine leaves and roots under cold treatment were examined via qRT-PCR. The transcripts levels of *VaERF057* progressively increased both in leaves and roots under cold treatment (Figure 1a), consistent with the previous findings (X. Sun et al. 2016). Phylogenetic analysis was conducted to elucidate the evolutionary relationship between *VaERF057* and *ERF* family members in *Arabidopsis*. The results revealed that VaERF057 belongs to group VII in the ERF family (Supporting Information S1: Figure 1). To determine the subcellular localisation of VaERF057, the 35S: GFP EV or 35S: VaERF057-GFP was transiently transformed

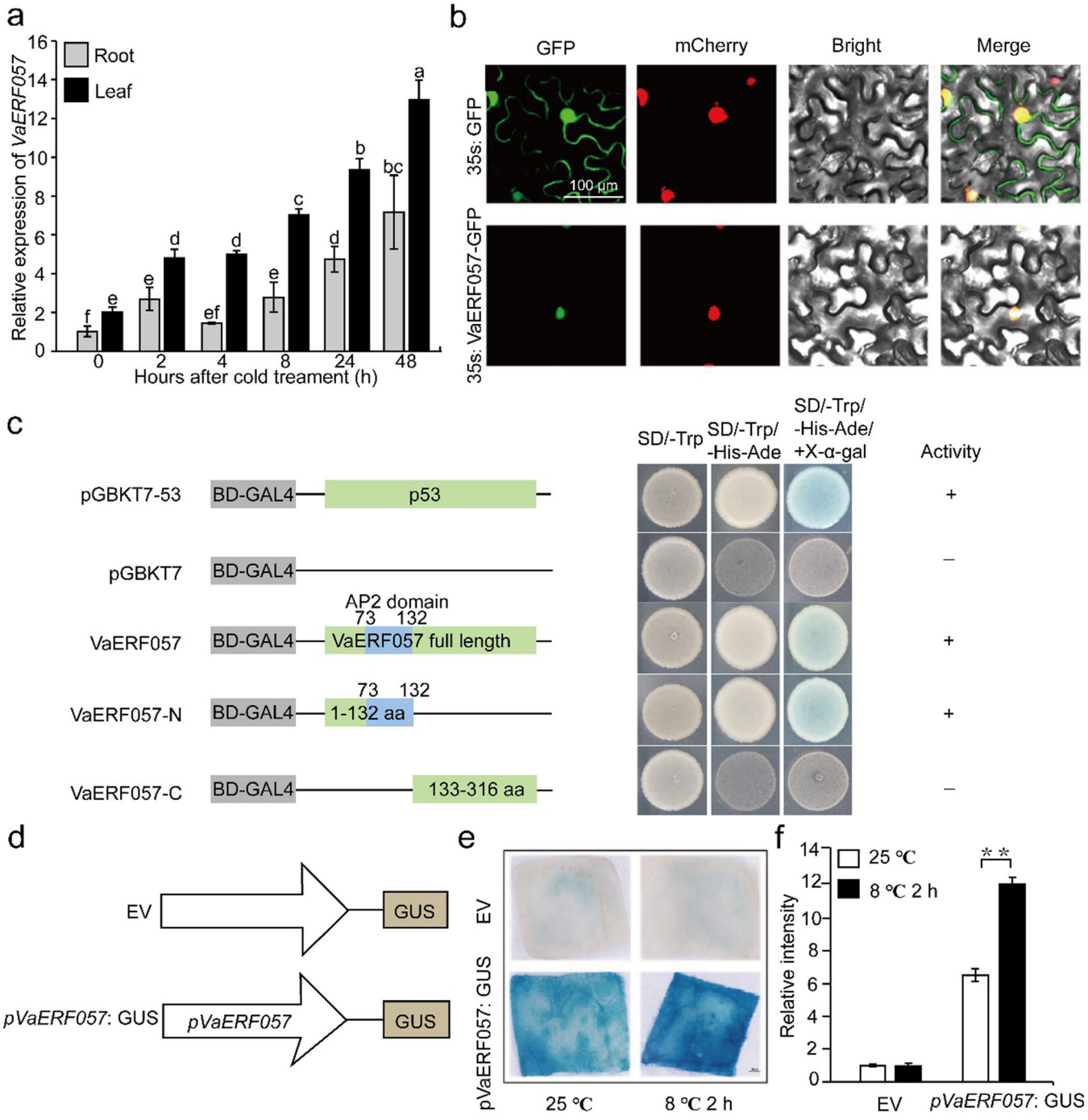

FIGURE 1 | *VaERF057* is a cold-inducible transcription factor localised in the nucleus with transcriptional activation activity. (a) Relative expression levels of *VaERF057* in grapevine leaves and roots under cold treatment were analysed. β-Actin (GenBank accession no. EC969944) was employed as an internal control. (b) Subcellular localisation of VaERF057. The fusion construct of 35S: VaERF057-GFP or 35S: GFP empty vector was co-introduced with a nucleus marker mCherry (VirD2NLS, Kumar and Kirti 2010) into *N. benthamiana* leaves. Epidermal cells imaging was performed using confocal microscopy with fluorescence signals detected in bright field, green (for GFP) and red (for mCherry) channels. Scale bars = 100 μm. (c) Schematic diagrams of vector constructions employed in transcriptional activity assays and corresponding growth of yeast cells co-transformed with distinct plasmid constructs on the selective medium, both in the presence and absence of X-α-gal. The full-length or truncated *VaERF057* (VaERF057-N and VaERF057-C represent constructs lacking the C-terminal domains or N-terminal domains, respectively) was fused into downstream of the GAL4 DNA-binding domain (DBD) in the pGBKT7 vector. The AP2 domain of VaERF057 is localised in 73–132 aa and marked with blue colour. The pGBKT7-53 served as the positive control, whereas the empty pGBKT7 vector was used as the negative control. (d) Schematic diagrams of vector constructions used for GUS assay. (e) GUS staining of transiently transformed tobacco leaves with EV or p*VaERF057*: GUS at 25°C and 8°C for 2 h. (f) GUS intensity of transformed tobacco leaves with EV or p*VaERF057*: GUS at 25°C and 8°C for 2 h. Error bars represent ± standard error ($n = 3$). Asterisks indicate significant differences between the vectors before and after the cold treatment (**$p < 0.01$). Different letters indicate significant differences ($p < 0.05$) according to Duncan's multiple range test. [Color figure can be viewed at wileyonlinelibrary.com]

into tobacco leaves via agroinfiltration. The fluorescence was found in both the cytoplasm and nucleus when transformed with EV, whereas VaERF057-GFP fusion protein exhibited fluorescence exclusively in the nucleus, as confirmed by its overlap with the red fluorescence from VirD2NLS-mRFP (nuclear maker) (Figure 1b). These results indicated that VaERF057 is localised in nuclear protein.

To investigate the transcriptional activation activity of VaERF057, a transactivation reporter assay was conducted using the full-length (1–316 aa) and two truncated fragments, either N-terminal (1–132 aa) or C-terminal (133–316 aa) (as shown in Figure 1c). Yeast cells exhibited robust growth on the SD/-Trp medium, whereas only constructs containing the full-length of VaERF057 and its N-terminal domain, as well as the positive control (pGBKT7-53), showed normal growth on the SD/-Trp/-His/-Ade + X-α-gal medium (Figure 1c). The findings supported that transcriptional activation activity of VaERF057 is localised to its N-terminal region.

The 2000-bp promoter sequences of *VaERF057* were inserted into GUS reporter system and transiently expressed in tobacco leaves (Figure 1d). Histochemical staining revealed that the tobacco leaves transformed with EV only show very weak GUS signal both at 25°C and 8°C for 2 h. The *pVaERF057*:GUS transformed leaves show the stronger GUS signal than control at 25°C, and signals are enhanced when the leaves are subjected to 8°C for 2 h (Figure 1e,f). These results further supported that *VaERF057* is a cold-inducible TF.

3.2 | *VaERF057* Functions Positively in Cold Stress Response in Grapevine

To verify the function of *VaERF057* during cold stress response, *VaERF057* was overexpressed in grapevine roots. The *VaERF057*-OE roots (#1–#3) exhibited higher transcript levels of *VaERF057* than the roots transformed with EV (Figure 2a).

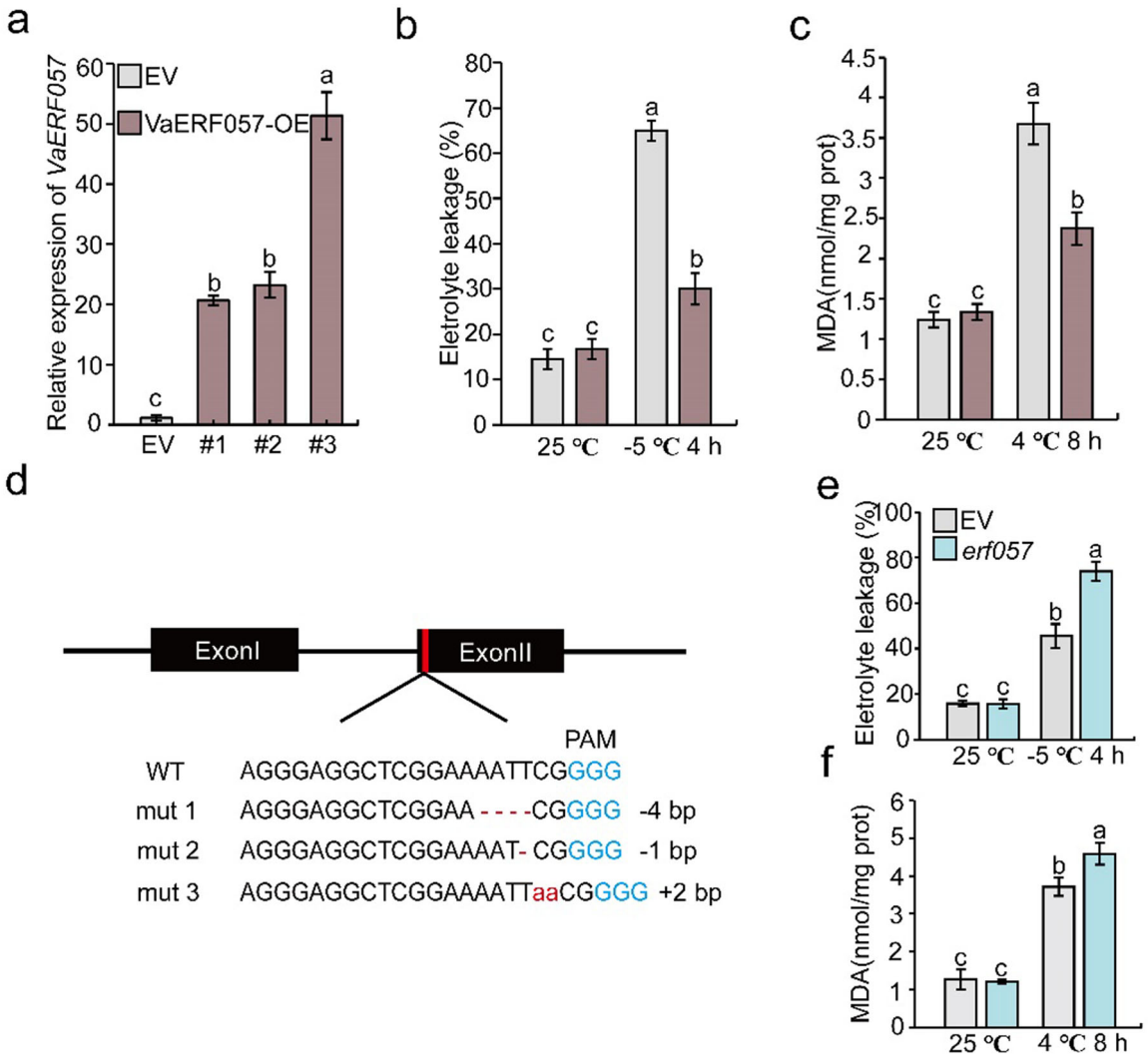

FIGURE 2 | The roles of *VaERF057* in cold stress response in grapevines. (a) qRT-PCR analysis validated the transcription level of *VaERF057* in EV and *VaERF057*-OE roots. (b) Electrolyte leakage (EL) in EV and *VaERF057*-OE roots at 25°C or −5°C for 4 h, respectively. (c) Malondialdehyde (MDA) in EV and *VaERF057*-OE roots at 25°C or 4°C for 8 h, respectively. (d) Hi-TOM sequencing results of *VaERF057* knock-out lines (*erf057*). The minus (−) symbol denotes the number of deleted nucleotides, and the red letters indicate the type of nucleotide inserted. (e) EL in EV and *erf057* roots at 25°C or −5°C for 4 h, respectively. (f) MDA content in EV and *erf057* roots at 25°C or 4°C for 8 h, respectively. Error bars represent ± standard error ($n = 3$). Different letters indicate significant differences ($p < 0.05$) according to Duncan's multiple range test. [Color figure can be viewed at wileyonlinelibrary.com]

VaERF057-OE and EV roots showed similar EL at 25°C (Figure 2b). After being subjected to freezing treatment at −5°C for 4 h, *VaERF057*-OE roots showed markedly lower EL levels compared to the EV roots (Figure 2b). *VaERF057*-OE lines also show less MDA content and ROS (H_2O_2 and $O_2^{\bullet-}$) than the EV roots at 4°C for 8 h (Figure 2c; Supporting Information S1: Figure 2a,b). These results indicated that OE of *VaERF057* increased cold tolerance in grapevine roots.

VaERF057 was knocked out in grapevine roots using CRISPR-Cas9 to further verify the function of *VaERF057* under cold stress. One target site that is located in 346–365 bp within the CDS of *VaERF057* was selected for editing. Hi-TOM sequencing confirmed the presence of mutations. The identified mutations comprised deletion and insertion events across three mutagenised root lines, specifically: a 4-bp deletion in mut1, a 1-bp deletion in mut2 and a 2-bp insertion in mut1. All of these mutations are anticipated to induce a translational frameshift, resulting in function-loss mutations (Figure 2d). Upon exposure to cold treatment (−5°C for 4 h), the *erf057* roots displayed higher EL levels compared to the EV roots (Figure 2e). In addition, the contents of MDA and ROS (H_2O_2 and $O_2^{\bullet-}$) were significantly higher in the *erf057* roots than those in the EV roots at 4°C for 8 h (Figure 2f; Supporting Information S1: Figure 3a,b), which indicated that KO of *VaERF057* decreased cold tolerance in grapevine roots.

Furthermore, VIGS was employed to downregulate the expression of *VaERF057* in the grapevine leaves. The transcription levels of *VaERF057* in the VIGS plants (defined as TRV-*VaERF057*) were significantly decreased in comparison to the control plants (defined as TRV, Supporting Information S1: Figure 4). No obvious phenotype can be found between the leaves of TRV-*VaERF057* and the control at 25°C. After freezing treatment at −5°C for 5 h, the leaves of TRV-*VaERF057* displayed wilting and then died, whereas the control only showed water-soaking in the leaves and growth well later (Figure 3a). The TRV-*VaERF057* lines show higher EL and MDA content together with H_2O_2 and $O_2^{\bullet-}$ levels compared to TRV control at −5°C for 5 h (Figure 3b,c; Supporting Information S1: Figure 5a,b). DAB and NBT stain results also show that the TRV-*VaERF057* leaves highly accumulate more H_2O_2 and $O_2^{\bullet-}$ content after cold treatment (−5°C for 5 h) than that in the control (Figure 3d). Altogether, these results illustrated the positive role of *VaERF057* under cold stress in the grapevine.

3.3 | *VaERF057* Binds to the Promoter of *VaFBA1* and Activates Its Expression

To explore the underlying mechanism by which *VaERF057* participates in the cold stress response in grapevine, DAP-seq was employed to systematically identify and characterise the downstream targets of *VaERF057*. Two replicates and a negative control were sequenced and named as VaERF057-1 (Rep1), VaERF057-2 (Rep2) and input, respectively. The DAP-seq analysis yielded 3.53 and 2.97 G of clean bases for Rep1 and Rep2, with filter efficiency rates of 99.26% and 99.30%, respectively. A total of 30 416 and 26 911 peaks were detected by VaERF057_1 and VaERF057_2, respectively, with 22 251 peaks overlapping between two replicates (Supporting Information S1: Figure 6a). The DNA-binding site of VaERF057 was predominantly distributed near the transcription start site (TSS) (Supporting Information S1: Figure 6b), where 19.39% of the DNA-binding sites were located within the 2-kb region upstream of the TSS (Supporting Information S1: Figure 6c,d). To identify significant motif sequences within peak regions, the MEME-ChIP tool from Multiple Em for Motif Elicitation (MEME) programme suite was employed. The most significant motif detected was "GGCGCC" (motif 1, E value $= 1.1 \times e^{-1489}$) followed by "GCCCAC" (motif 2, E value $= 1.9 \times e^{-597}$), respectively (Figure 4a).

Since too many candidate targets were found by DAP-seq, the RNA-seq data were generated using *VaERF057*-OE and EV roots. A total of 768 upregulated genes were found in *VaERF057*-OE roots when compared with the control. Among these genes, only 144 genes show VaERF057-binding peaks in the promoter regions from DAP-seq results (Supporting Information S1: Figure 6e). The KEGG pathways analysis showed that carbohydrate metabolism is enriched within 144 genes, which implied the putative pathway regulated by *VaERF057* during the cold stress response in grapevines (Supporting Information S1: Figure 6f).

To gain deeper insight into the downstream genes of *VaERF057*, the expression pattern of 144 candidate genes under cold stress was grabbed from previously published transcriptome data (Xin et al. 2013). Only eight genes exhibited low-temperature-induced expression patterns (Supporting Information S2: Table 4). One of the genes annotated as *fructose-bisphosphate aldolase 1* (*VaFBA1*, Supporting Information S1: Figure 7a) was found to increase progressively under cold treatment in leaves and roots in grapevine (Supporting Information S1: Figure 7b,c). Two candidate VaERF057-binding cis-element, GCCCAC, were found in the promoter of *VaFBA1* (arrow in Figure 4b) and the DAP-seq peaks near this element were higher in ERF057-1 and ERF057-2 than in input (Figure 4b). Thus, *VaFBA1* was chosen as a candidate downstream gene for the following analysis.

Y1H was conducted to investigate whether VaERF057 can interact with GCCCAC elements. The yeast cells coexpressed with prey and the bait harbouring the wild-type *VaFBA1* promoter fragment, which includes two GCCCAC sequences, exhibited normal growth on the AbA-supplemented medium. In contrast, when the GCCCAC was mutated into AAAAAA, the growth of yeast was completely inhibited (Figure 4c). The EMSA demonstrated that a specific mobility shift was detected when the His-VaERF057 fusion protein was incubated with the labelled probe harbouring the GCCCAC sequence. The addition of unlabelled competitor DNA into the reaction mixture caused concentration-dependent suppression of band shift intensity. Moreover, mutation of the GCCCAC sequence resulted in the complete abolition of the observed band shift, which suggested that the putative transcriptional regulation of VaERF057 by binding to the GCCCAC sequence within the promoter regions of *VaFBA1* (Figure 4d).

We then performed a LUC to investigate the transcriptional activation of the *VaFBA1* promoter by VaERF057. The CaMV*35S* promoter-driven VaERF057 was used as an effector,

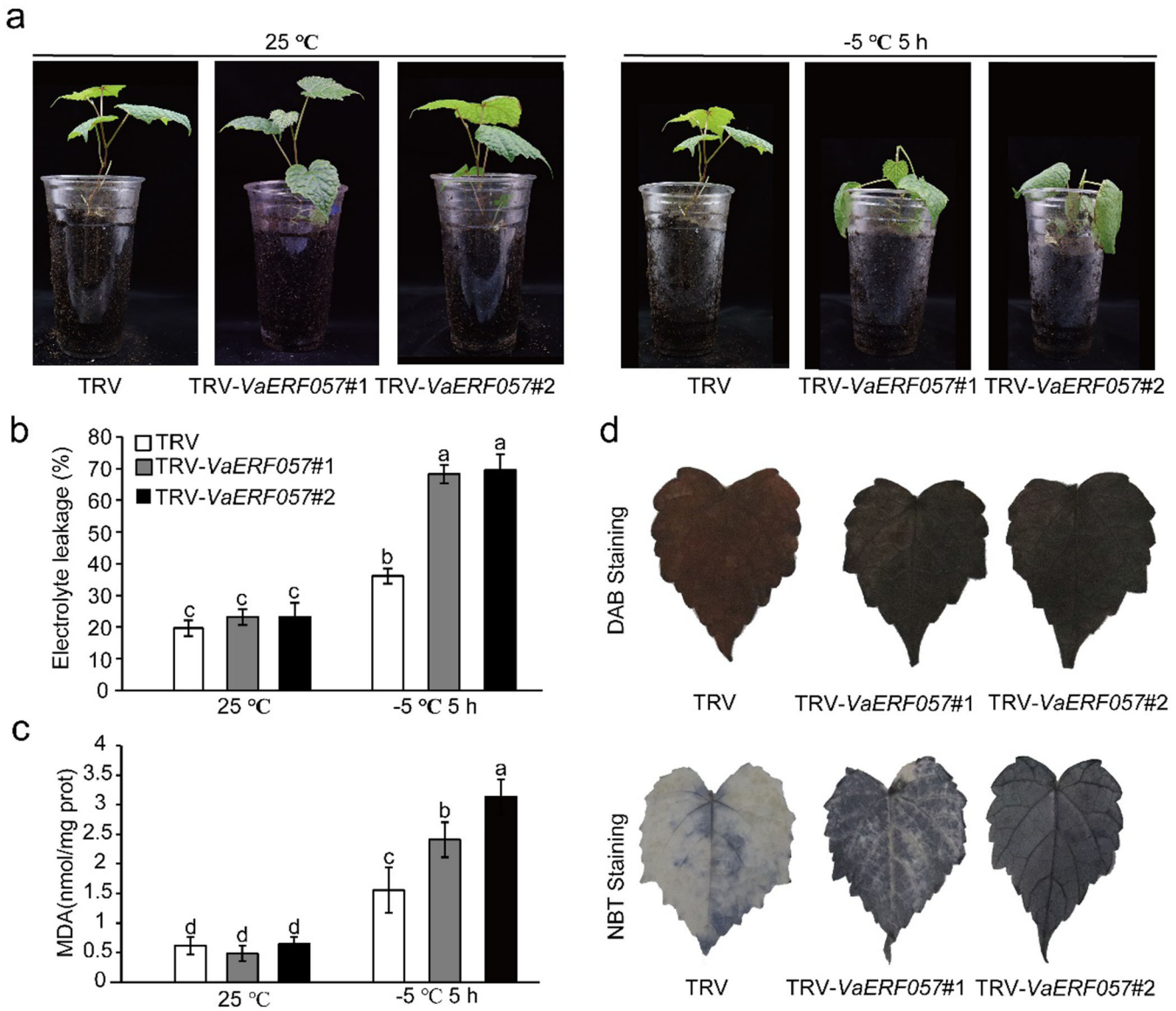

FIGURE 3 | Silencing of *VaERF057* by virus-induced gene silencing (VIGS) decreased the cold tolerance of grapevine leaves. (a) The phenotypes of control (TRV) and TRV-*VaERF057* at 25°C and −5°C for 5 h. (b, c) Percentage of electrolyte leakage and MDA in TRV and TRV-*VaERF057* leaves at 25°C and −5°C for 5 h. (d) In situ detection of H_2O_2 and $O_2^{\cdot-}$ in TRV control and TRV-*VaERF057* leaves after cold treatment at −5°C for 5 h, visualised by DAB and NBT histochemical staining, respectively. Error bars represent ± standard error ($n = 3$). Different letters indicate significant differences ($p < 0.05$) according to Duncan's multiple range test. [Color figure can be viewed at wileyonlinelibrary.com]

whereas the LUC reporter gene was fused in frame with the promoter or mutant promoter of *VaFBA1* (Figure 4e). The results from quantitative dual LUC assay and LUC fluorescence observation showed that VaERF057 activated the reporter genes when GCCCAC element was in *VaFBA1* promoter, whereas the fluorescence was weakened when GCCCAC element was mutated into AAAAAA (Figure 4f). Together, these results indicated that VaERF057 activates the expression of *VaFBA1* through interaction with GCCCAC element.

3.4 | *VaERF057* Regulates the Expression of *VaFBA1* and Sugar Metabolism

The above results indicated that *VaFBA1* may be one of the targets of VaERF057. The expressions of *VaFBA1* and soluble sugar contents were further analysed in *VaERF057*-OE roots, *erf057* roots and TRV-*VaERF057* leaves. The transcription levels of *VaFBA1* were increased in *VaERF057*-OE roots, but decreased in *erf057* roots and TRV-*VaERF057* leaves when compared to the control, respectively (Figure 5a–c). The soluble sugar contents were increased in *VaERF057*-OE roots, whereas decreased in the KO and VIGS lines under 25°C or cold treatment in comparison to controls (Figure 5d–f). These results indicated that VaERF057 modulates soluble sugar metabolism by regulating the expression of *VaFBA1*.

3.5 | *VaFBA1* Functions Positively During Cold Stress by Regulating Sugar Metabolism

The functions of *VaFBA1* in cold stress response and sugar metabolism were further detected by OE, KO and VIGS systems in

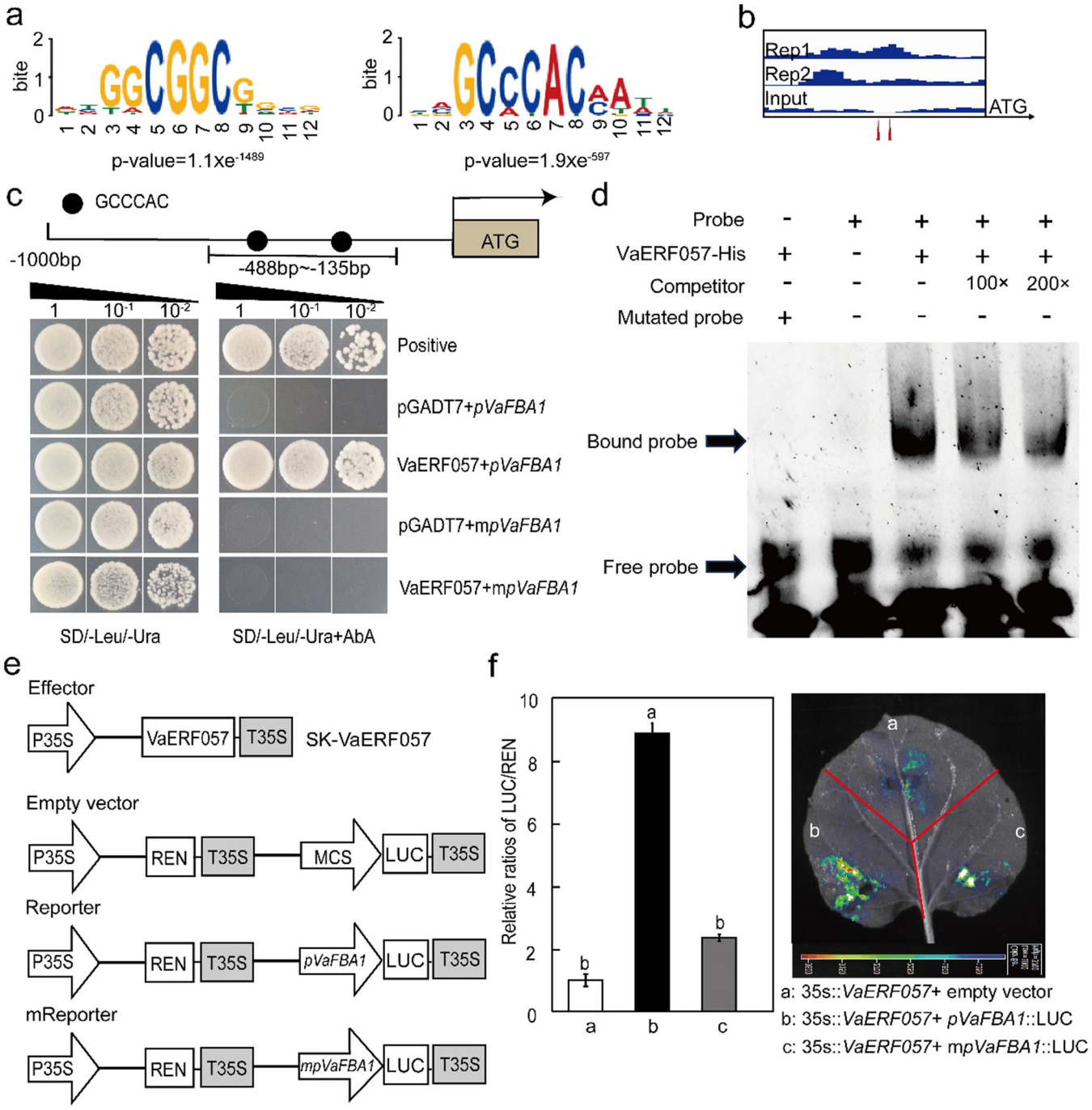

FIGURE 4 | Identification of the cis-element and downstream gene of *VaERF057*. (a, b) The potential cis-element recognised by VaERF057 from DAP-seq results. (b) Peaks close to the two GCCCAC sequences in the promoter regions of *VaFBA1*. (c) Yeast cells harbouring various prey–bait combinations were cultured on selective medium in the absence or presence of Aureobasidin A (AbA). (d) EMSA analysis of specific interaction between VaERF057 and the GCCCAC motif within the *VaFBA1* promoter. The purified His-VaERF057 protein was subjected to binding assays with 5-carboxyfluorescein (5-FAM) labelled containing the wild-type or AAAAAA (mutated GCCCAC element). Unlabelled probes were used as a competitor. + and − denote the presence and absence of the components in each reaction, respectively. (e) Structural diagrams of effector and reporter constructs used for dual-luciferase assay. (f) Relative ratios of LUC/REN and representative bioluminescence image co-transformed with different reporters and effectors in the tobacco leaves. LUC denotes firefly luciferase, and REN indicates *Renilla* luciferase. Error bars represent ± standard error ($n = 3$). Different letters indicate significant differences ($p < 0.05$) according to Duncan's multiple range test. [Color figure can be viewed at wileyonlinelibrary.com]

grapevine. The *VaFBA1*-OE roots show an increased transcription level of *VaFBA1* (Figure 6a). After exposure to −5°C for 4 h, the EL levels of *VaFBA1*-OE lines were significantly lower than the EV control (Figure 6b). Additionally, *VaFBA1*-OE lines also show lower MDA and ROS (H_2O_2 and $O_2^{\bullet-}$) content than EV roots after incubating at 4°C for 8 h (Figure 6c; Supporting Information S1: Figure 8a,b). These results suggested that OE of *VaFBA1* increased cold tolerance in the grapevine.

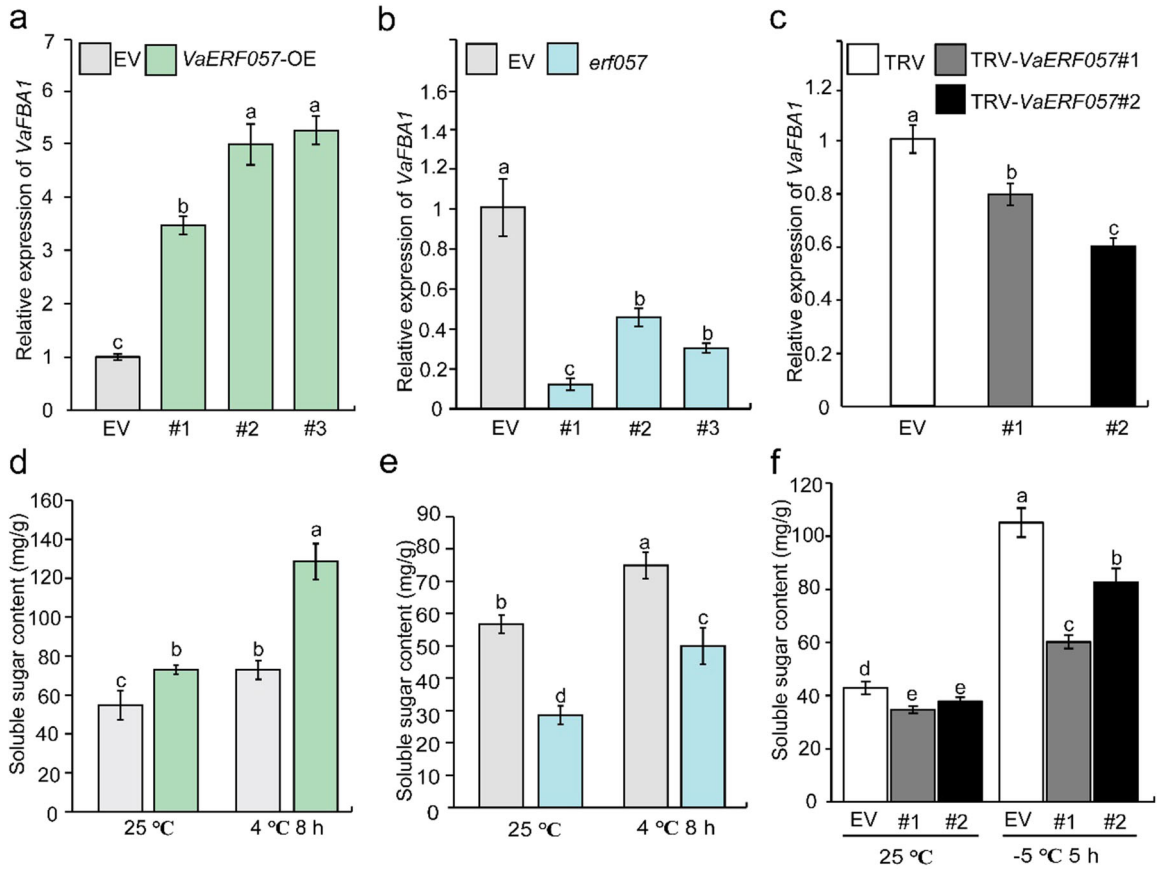

FIGURE 5 | *VaERF057* is involved in sugar metabolism by regulating *VaFBA1*. Relative expression of *VaFBA1* in *VaERF057*-OE roots (a), *erf057* roots (b) and TRV-*VaERF057* leaves (c) by qRT-PCR. (d, e) Soluble sugar content in *VaERF057*-OE roots (d), *erf057* roots (e) at 25°C or 4°C for 8 h, respectively. (f) Soluble sugar content in TRV-*VaERF057* leaves at 25°C or −5°C for 5 h. Error bars represent ± standard error ($n = 3$). Different letters indicate significant differences ($p < 0.05$) according to Duncan's multiple range test. [Color figure can be viewed at wileyonlinelibrary.com]

To confirm the role of *VaFBA1* during the cold stress response, the *fba1* KO roots were generated by CRISPR-Cas9. One target site that is located in 118–137 bp in the CDS of *VaFBA1* was selected for editing. Hi-TOM sequencing confirmed the presence of mutations. The mutations include deletions/insertions in three mutagenised plants (mut 1: 1 bp insertions; mut 2: 1 bp deletion; mut 3: 1 bp deletion). All of these mutations are anticipated to cause a frameshift, resulting in function-loss mutation (Figure 6d). Upon exposure to the aforementioned cold treatment, the *fba1* roots displayed elevated EL, the MDA and ROS (ROS, H_2O_2 content and $O_2^{\bullet-}$ content) levels compared to EV roots, respectively (Figure 6e,f; Supporting Information S1: Figure 9a,b).

The VIGS system was also used to generate knockdown leaves, and the decreased expression of *VaFBA1* was confirmed by qRT-PCR in TRV-*VaFBA1* (Supporting Information S1: Figure 10a–c). No obvious phenotype was found in TRV-*VaFBA1* leaves at 25°C. After freezing treatment at −5°C for 5 h, the leaves of TRV-*VaFBA1* displayed wilting and then died, whereas the control only showed water-soaking in the leaves and growth well later (Figure 7a). The TRV-*VAFBA1* leaves also show weak cold hardiness with higher EL, MDA and ROS levels (Figure 7b,c; Supporting Information S1: Figure 11a,b). DAB and NBT stain results show the TRV-*VaFBA1* leaves accumulated more H_2O_2 and $O_2^{\bullet-}$ content after cold treatment (−5°C for 5 h) than that in control (Figure 7d). These findings are consistent with those of KO roots as described above, which demonstrated that *VaFBA1* positively contributed to the cold tolerance of the grapevine.

The soluble sugar content was determined in OE roots, KO roots and knockdown leaves, respectively. A notable increase in sugar content was observed in the *VaFBA1*-OE roots after cold treatment at 4°C for 8 h (Supporting Information S1: Figure 12a). While soluble sugar content decreased in the KO and VIGS lines under normal or cold treatment when compared with controls (Supporting Information S1: Figure 12b,c). These findings support the positive roles of *VaFBA1* in cold stress response by increasing the soluble sugar content in the grapevine.

3.6 | VaEIN3.1 Is a Cold-Inducible TF That Can Bind to the Promoter of *VaERF057*

Previous results demonstrated that *VaERF057* is induced by ethylene during cold treatment (X. Sun et al. 2016). To investigate how ethylene induces the expression of *VaERF057*, we analysed the promoter of *VaERF057* and found that there are EIN3/EIL-binding sites (EBS, core sequence: ATGTA) (Figure 8a). By using the amino acid sequences of EIN3/EIL from *Arabidopsis*, a total of four EIN3/EILs were identified from the grapevine genome (PN40024), including *VaEIN3.1* (*VIT_ 213s0047g00250*), *VaEIN3.2*

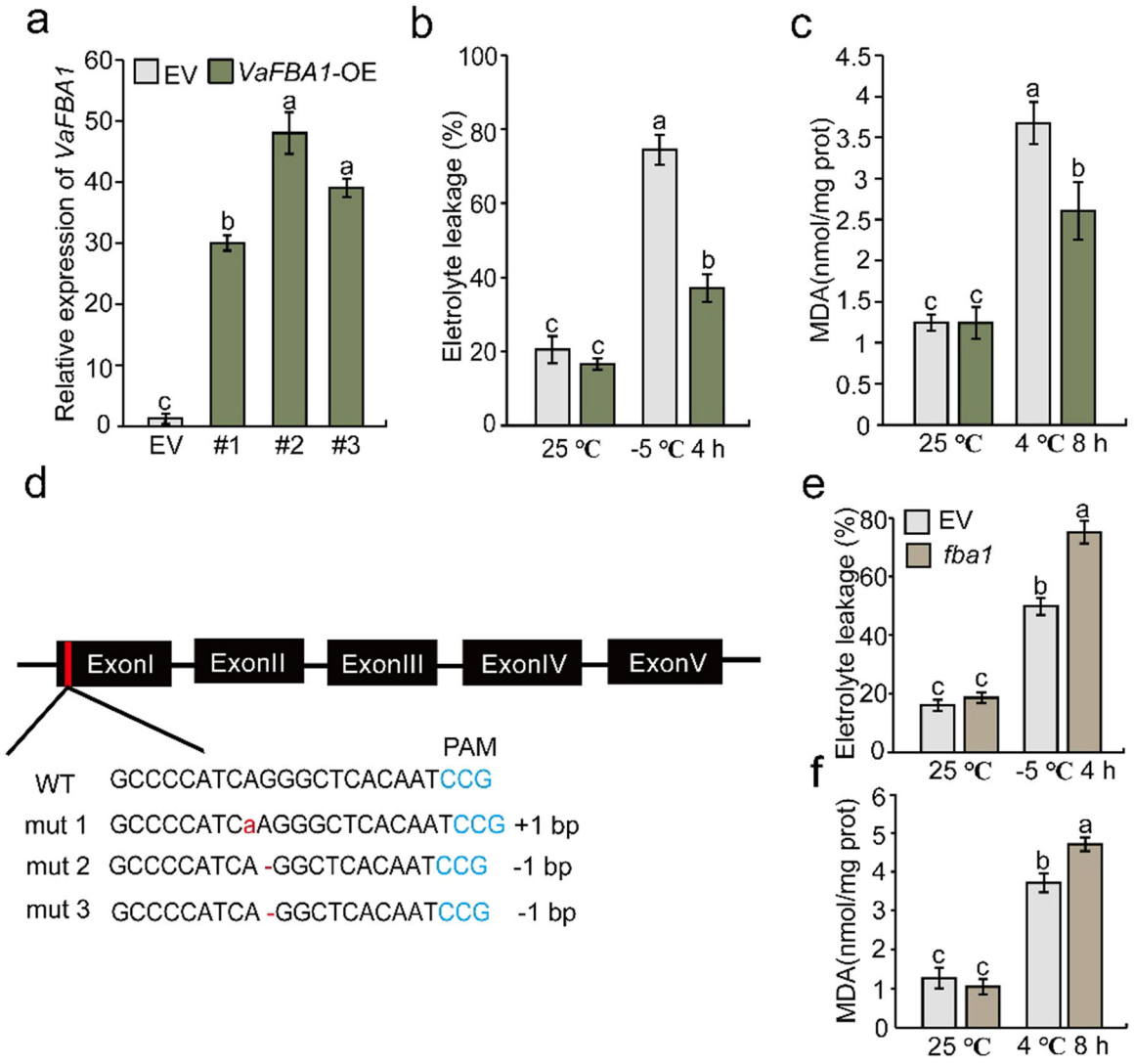

FIGURE 6 | The role of *VaFBA1* in cold stress response in grapevine. (a) qRT-PCR analysis verified the transcription level of *VaFBA1* in EV and *VaFBA1*-OE roots. (b) Electrolyte leakage in EV and *VaFBA1*-OE roots at 25°C or −5°C for 4 h, respectively. (c) Malondialdehyde (MDA) was measured in EV and *VaFBA1*-OE roots at 25°C or 4°C 8 h, respectively. (d) Hi-TOM sequencing results of *VaFBA1* knock-out lines (*fba1*). The minus (−) symbol denotes the number of deleted nucleotides, and the red letters indicate the type of nucleotide inserted. (e) Electrolyte leakage measured in EV and *fba1* roots at 25°C or −5°C for 4 h, respectively. (f) MDA content in EV and *fba1* at 25°C or 4°C for 8 h, respectively. Error bars represent ± standard error ($n = 3$). Different letters indicate significant differences ($p < 0.05$) according to Duncan's multiple range test. [Color figure can be viewed at wileyonlinelibrary.com]

(*VIT_206s0009g01380*), *VaEIL3* (*VIT_206s0004g01610*) and *VaEIL4* (*VIT_200s0357g00120*) (Supporting Information S1: Figure 13a). RNA-seq data from cold and cold + AVG (ethylene synthesis inhibitor) treatment leaves of grapevine (Hou et al. 2023) showed that only the expression of *VaEIN3.1* increased under low temperature, and the trend was inhibited by AVG (Supporting Information S1: Figure 13b). To confirm this finding, the expression of *VaEIN3.1* was examined in *V. amurensis*. The qRT-PCR analysis demonstrated that *VaEIN3.1* was highly expressed during the cold treatment. However, their expression levels decreased significantly under cold + AVG treatment (Supporting Information S1: Figure 13c). These results indicated that *VaEIN3.1* is an ethylene-dependent cold-inducible TF.

To determine whether VaEIN3.1 directly interacts with the *VaERF057* promoter and regulates its expression, Y1H, EMSA and LUC assays were conducted. Y1H was used to check if VaEIN3.1 can bind to the EBS element. As shown in Figure 8a, the yeast coexpressed with prey and bait vectors harbouring *VaERF057* promoter with ATGTA sequence exhibited normal growth on the AbA-supplemented medium. In contrast, when the ATGTA sequence was mutated to CCCCC, yeast cells failed to grow under the same conditions. The EMSA identified a specific mobility shift when VaEIN3.1-His fusion protein was incubated with labelled probe containing the ATGTA sequence. The addition of unlabelled competitor DNA into the reaction mixture caused a concentration-dependent suppression of band shift intensity. Moreover, mutation of the ATGTA sequence resulted in the complete abolition of the observed band shift, which suggested that VaEIN3.1 can bind directly and specifically to the ATGTA sequence within the *VaERF057* promoter (Figure 8b). Then, LUC was performed to investigate the transcriptional regulation of *VaERF057* by VaEIN3.1. VaEIN3.1 was driven by the CaMV*35S* promoter and used as an effector. The

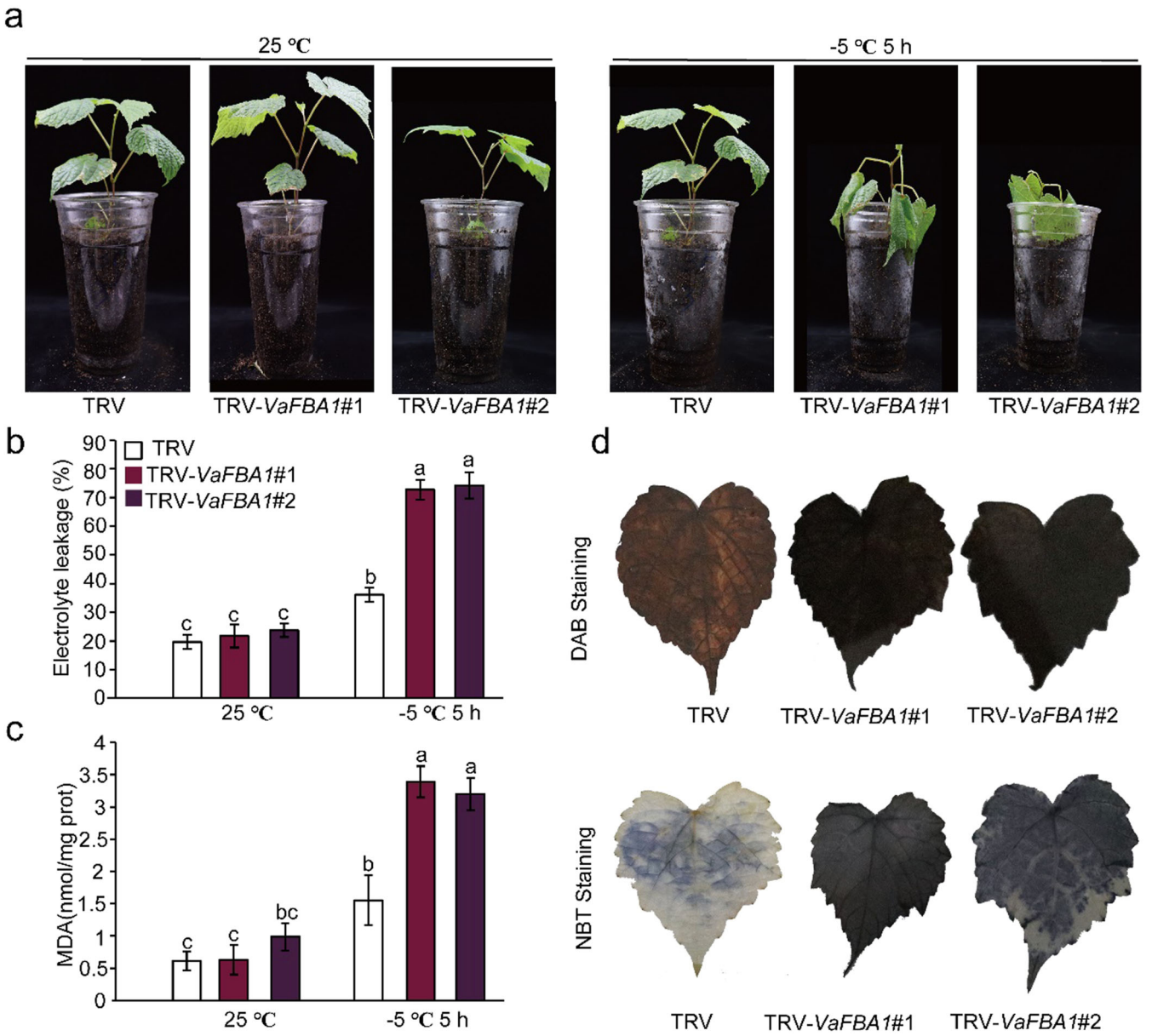

FIGURE 7 | Silencing of *VaFBA1* elevates cold sensitivity of *V. amurensis*. (a) The phenotypes of TRV plants and TRV-*VaFBA1* plants at 25°C and −5°C 5 h. (b, c) Electrolyte leakage (b) and MDA content (c) in TRV control and TRV-*VaFBA1* plants at 25°C and −5°C for 5 h. (d) In situ detection of H_2O_2 and $O_2^{\cdot-}$ in TRV control and TRV-*VaFBA1* plants after cold treatment at −5°C 5 h, visualised by DAB and NBT histochemical staining, respectively. Error bars represent ± standard error ($n = 3$). Different letters indicate significant differences ($p < 0.05$) according to Duncan's multiple range test. [Color figure can be viewed at wileyonlinelibrary.com]

LUC reporter gene was fused in frame with the normal or mutant promoter of *VaERF057* (Figure 8c). The results showed that VaEIN3.1 activated *VaERF057* by interacting with the ATGTA element in the promoter (Figure 8d). Those results clearly showed that VaEIN3.1 can bind to the promoter of *VaERF057* and activate its expression.

3.7 | VaEIN3.1 Controls the *VaERF057-VaFBA1* Module Under Cold Condition

To check the contribution of *VaEIN3.1* in cold stress response in grapevine, *VaEIN3.1*-OE roots were generated by *A. rhizogenes*-induced transformation system (Supporting Information S1: Figure 15a). After exposure to −5°C for 4 h, the *VaEIN3.1*-OE lines exhibited significantly lower EL levels compared to the EV control plants (Supporting Information S1: Figure 15b). After exposure to 4°C for 8 h, the *VaEIN3.1*-OE lines demonstrated significantly lower MDA levels compared to the EV control plants (Supporting Information S1: Figure 15c). To further investigate the role of *VaEIN3.1* in cold stress, we constructed a TRV-*VaEIN3.1* vector to specifically silence *VaEIN3.1* expression in grapevine (Supporting Information S1: Figure 14a–c). No obvious phenotypic was observed under normal growth conditions between the control and VIGS plants. The TRV-*VaEIN3.1*-silenced plants showed wilting phenotypes at −5°C for 5 h compared to TRV control (Supporting Information S1: Figure 15d). The EL, MDA and ROS (H_2O_2 content by DAB

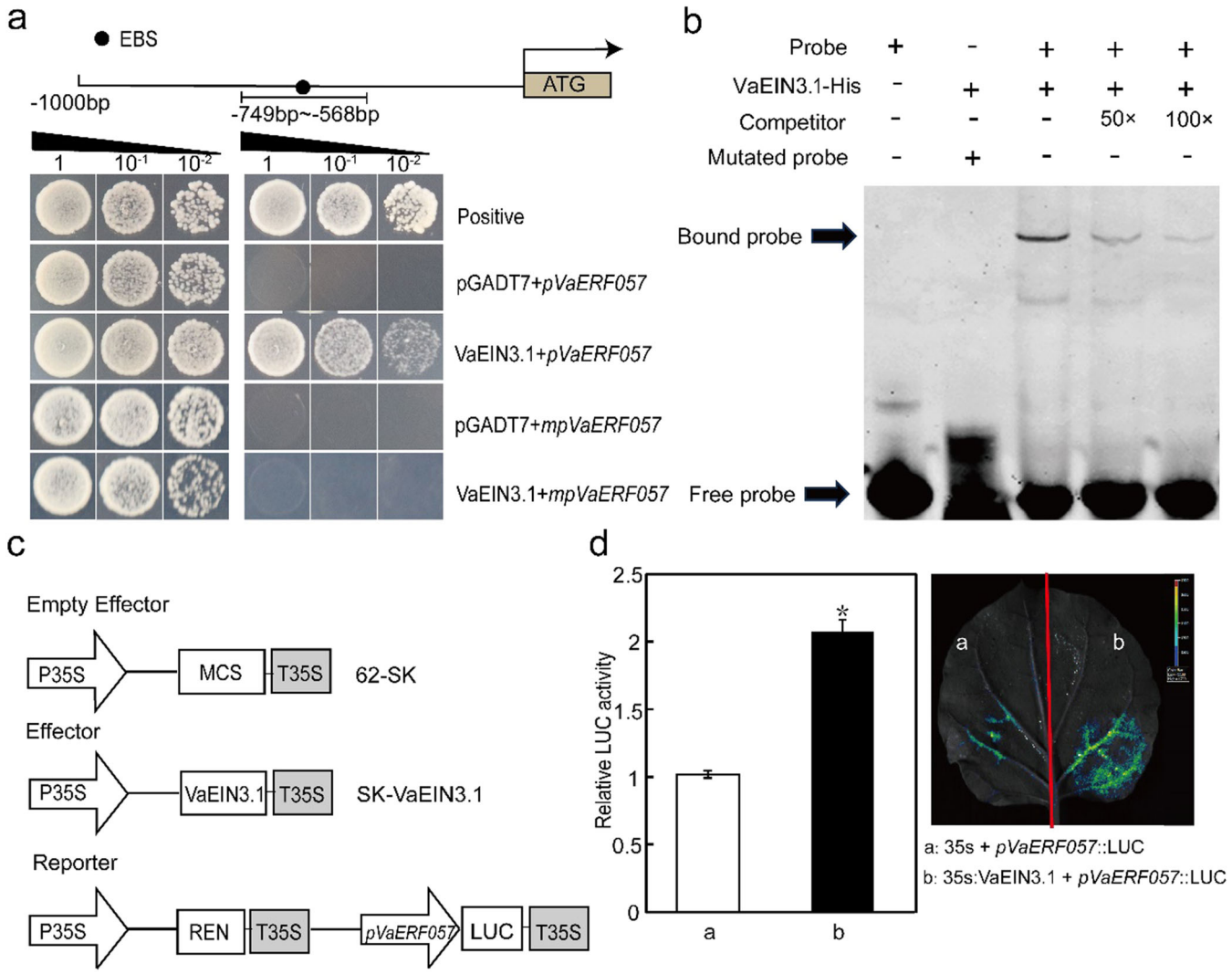

FIGURE 8 | VaEIN3.1 binds to the *VaERF057* promoter and positively regulates its expression. (a) Yeast cells harbouring various prey–bait combinations were cultured on selective medium in the absence or presence of Aureobasidin A (AbA). (b) EMSA analysis of specific interaction between VaEIN3.1 and the EBS motif within the *VaERF057* promoter. The purified His-VaEIN3.1 protein was subjected to binding assays with 5-carboxyfluorescein (5-FAM) labelled containing the wild-type or mutated CCCCC element. Unlabelled probes were used as a competitor. + and − denote the presence and absence of the components in each reaction, respectively. (c) Structural diagrams of effector and reporter constructs used for dual-luciferase assay. (d) Relative ratios of LUC/REN and representative bioluminescence image co-transformed with different reporters and effectors in the tobacco leaves. LUC denotes firefly luciferase, and REN indicates *Renilla* luciferase. Error bars represent ± standard error ($n = 3$). Asterisks indicate significant differences between the vectors before and after the cold treatment ($^*p < 0.05$). [Color figure can be viewed at wileyonlinelibrary.com]

staining and $O_2^{\bullet-}$ content by NBT staining) levels of the TRV-*VaEIN3.1*-silenced plants were higher than TRV control (Supporting Information S1: Figure 15e–g). These results supported the positive role of *VaEIN3.1* in cold stress response in the grapevine.

To discover the regulation of VaEIN3.1 on the *VaERF057-VaFBA1* module during low temperature, the gene expression as well as the sugar content was detected in *VaEIN3.1*-OE and TRV-*VaEIN3.1* material as mentioned above. Both the expression levels of *VaERF057* and *VaFBA1* and sugar content in *VaEIN3.1*-OE roots increased when compared with EV roots (Figure 9a–c). When the expression of *VaEIN3.1* was knocked down in the grapevine leaves, the expression levels of *VaERF057* and *VaFBA1* and the sugar content were lower in TRV-*VaEIN3.1* leaves than in control (Figure 9d–f). Taken together, these results support the contribution of the VaEIN3.1-VaERF057-VaFBA1 module to the cold tolerance in grapevine by adjusting the soluble sugar content.

4 | Discussion

The AP2/ERF TFs have been recognised as key regulators in adapting to a variety of abiotic stress conditions in plants, such as low temperature, drought and salinity in plants (Xie et al. 2019; Meng et al. 2020; Kong et al. 2023; L. Xu et al. 2024). The physiological and molecular mechanisms of *ERF* functions under cold stress, especially in perennial plants like grapevine, are not well understood. *VaERF057* is one of the *ERFs* that

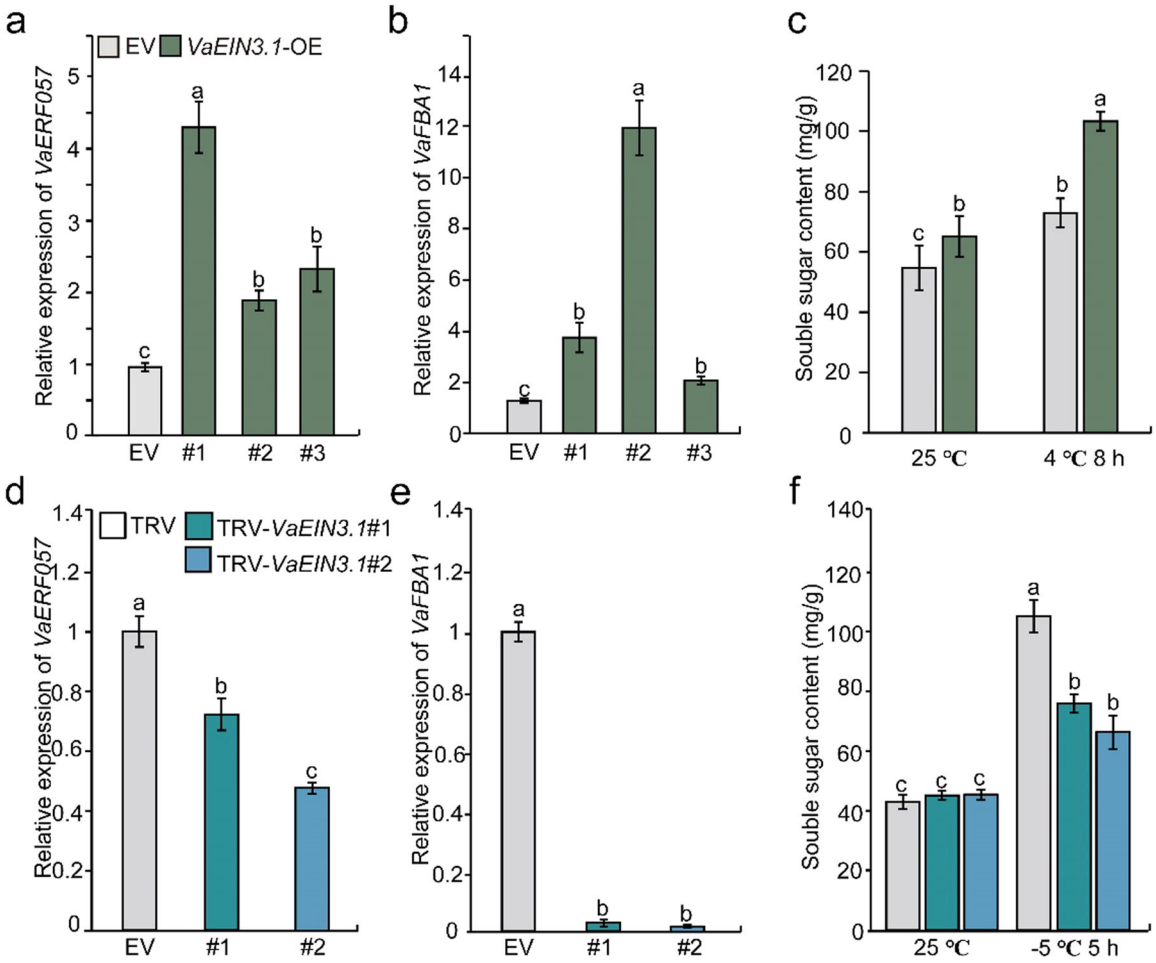

FIGURE 9 | VaEIN3.1 is involved in sugar metabolism by regulating *VaERF057* and *VaFBA1*. (a, b) Relative expression of *VaERF057* (a) and *VaFBA1* (b) in *VaEIN3.1*-OE plants by qPCR. (c) Sugar content in *VaERF057*-OE plants at 25°C and 4°C 8 h. (d, e) Relative expression of *VaERF057* (d) and *VaFBA1* (e) in *VaEIN3.1* VIGS plants by qPCR. (f) The sugar content of *VaEIN3.1* VIGS plants at 25°C and −5°C 5 h. Error bars represent ± standard error ($n = 3$). Different letters indicate significant differences ($p < 0.05$) according to Duncan's multiple range test. [Color figure can be viewed at wileyonlinelibrary.com]

respond to cold stress treatment in the grapevine. Here, we discovered the pathways that *VaERF057* is involved during cold stress responses. The findings may not only contribute to the identification of *VaERF057* as a valuable member of the cold-responsive gene used for genetic engineering but also help to uncover the whole network that is regulated by ethylene during cold stress response in grapevine.

To date, the direct downstream targets of ERFs and related biological processes have been identified in plants that subjected to different stresses. In *Populus tomentosa*, *PtoERF15* was found to improve drought tolerance in maintaining stem water potential by regulating PtoMYC2b to modulate xylem vessel development (Kong et al. 2023). The SmAP2-17 functions as a positive regulator during salt stress by upregulating SOS3 and ABI5 in *Salix matsudana* (Y. Chen et al. 2022). CmERF5 specifically interacts with GCC-like motifs within the promoter region of *CmRAP2.3* and activates its expression to alleviate waterlogging stress through the ROS-mediated pathway in chrysanthemum (C. Li et al. 2023). In tomato, ERF15 was found to enhance cold tolerance via regulating *CBF* and *WRKY6* (Hu et al. 2024). OsERF52 was identified as a positive modulator in response to low temperatures by directly regulating the expression of *CBF* genes (L. Xu et al. 2024). However, the direct transcriptional regulation of *FBA* genes by ERFs remains unreported. Here, the identification of *VaFBA1* as a direct target of VaERF057 offers valuable insights into the ERF regulon involved in abiotic stress responses. This finding may shed new light on the regulatory cascades of dynamic sugar metabolism, a phenomenon commonly observed when plants are subjected to cold or other environmental stresses (Han et al. 2020; Liang et al. 2024).

It is still a big challenge to find the direct target from a large number of candidates based on a single method. Here, both transcriptome and DAP-seq were used to identify the downstream genes of *VaERF057*. The gene list obtained by overlapping upregulated DEGs and accumulated DAP-seq peaks in the promoter regions was further filtered by upregulated expression pattern under cold treatment in grapevine leaves. Except for *VaFBA1*, other candidate genes such as calmodulin-like proteins (CMLs) are also worth studying in the future. CMLs are multifunctional proteins that have Ca^{2+}-binding capacity (Yamaguchi et al. 2005; S. Liu et al. 2024). CMLs play a critical role in Ca^{2+} signalling during plant adaptations to abiotic stress in plants (Magnan et al. 2008; Park et al. 2010; G. Y. Xu

et al. 2011; Munir et al. 2016). For example, *MtCML42* regulates cold tolerance through upregulating the *CBF* signalling pathway and downregulating *MtABI5* (Q. Sun et al. 2021). In addition, VaERF057-OE transcriptome and DAP-seq data also indicated other pathways such as phenylpropanoid biosynthesis and amino acid metabolism that VaERF057 may involve in. Recent studies have shown that phenylpropanoid plays a significant role in cold stress response in plants. For example, in *Artemisia annua*, cold stress significantly upregulated the accumulation of flavonoids and lignin and led to enhanced cold tolerance by providing structural support and antioxidant protection (He et al. 2024). Prestorage CA induced the expression of genes in the phenylpropanoid pathway and contributed to the chilling tolerance in cucumber fruits (B. Wang et al. 2021). Further works are still needed to confirm that whether *VaERF057* regulates phenylpropanoid biosynthesis and amino acid metabolism during cold stress response in grapevine.

Soluble sugars function not only as essential energy substrates but also as multifunctional molecules, act as cryoprotectants, antioxidants and signalling mediators (Dahro et al. 2016; Nakabayashi and Saito 2015; T. Peng et al. 2014). The soluble sugar homeostasis and the relevant gene expression are crucial determinants of plant performance and survival under cold stress. PtrERF110 was found to elevate the levels of sugars and sterols by activating genes such as *PtrERD6L16*, *PtrSPS4* and *PtrUGT80B1*, thereby enhancing its cold tolerance (Khan et al. 2024). MrERF039 has been shown to enhance the glucose and maltose content as well as cold tolerance by modulating the expression of various sugar transporters and sugar metabolism-related genes in *Medicago ruthenica* root (Fu et al. 2024). Studies in several plants have clearly demonstrated the critical role of *FBA*s in modulating plant stress tolerance, growth and development. Although the expression of *FBAs* was found to increase during cold stress in many species (Mu et al. 2021; K. Peng et al. 2022; S. Yu et al. 2022), the transcriptional regulation mechanism remains unclear. Here, the integrative analyses revealed that VaERF057 specifically binds to the GCCCAC cis-element within the *VaFBA1* promoter region, thereby directly activating its transcription. This is the first report about the transcriptional regulation of an *FBA* gene by an ERF protein. The VaERF057-VaFBA1 module in this study provides new links between soluble sugar metabolism and ethylene signalling during cold stress response in plants.

In addition, we also found that the *VaERF057*-OE roots accumulated significantly less ROS, whereas ROS content was noticeably increased in the *VaERF057*-KO roots or the VIGS plants. It had been reported that soluble sugars participate in or associated with the generation of ROS. Conversely, soluble sugars also contribute to ROS scavenging by producing NADPH. The NADPH serves as a critical cofactor during ROS scavenging by ascorbate-glutathione cycle (Couée et al. 2006). Therefore, it was assumed that the lower ROS levels in *VaERF057* roots may be partly due to the increased soluble sugar contents.

Ethylene exhibits different regulatory effects on cold tolerance, acting as either an enhancer or suppressor depending on the plant species (Shi et al. 2012; Y. Zhang et al. 2022). In grapevines, the ethylene synthesis rate increased during low-temperature treatment (X. Sun et al. 2016). Moreover,

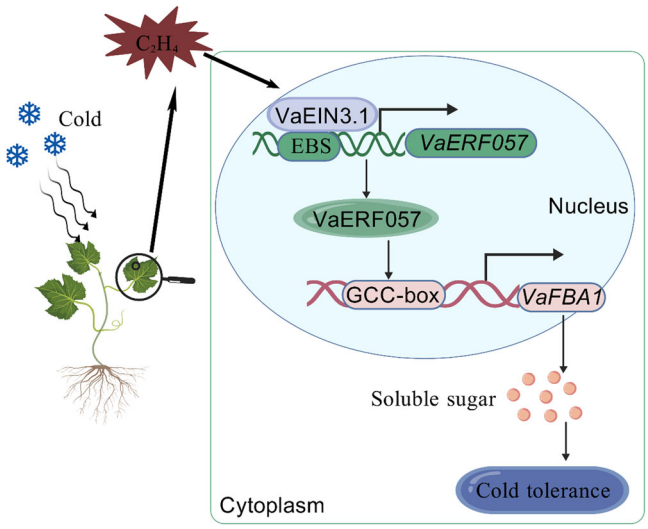

FIGURE 10 | VaEIN3.1-VaERF057-VaFBA1 module regulates the soluble sugar content under cold stress in grapevine. [Color figure can be viewed at wileyonlinelibrary.com]

exogenous treatment with ACC, the biosynthetic precursor of ethylene, significantly improved cold tolerance, whereas exogenous application of AVG, the biosynthetic inhibitor of ethylene, reduced the cold tolerance. These findings indicated that ethylene functions as a key positive regulator in improving cold tolerance in grapevine. The rapid induction of *VaERF057* in grapevine led us to explore how ethylene mediated regulation of *VaERF057* expression. The EIN3/EILs homologues, known as key positive regulators in the ethylene signal cascade, have been extensively studied in various plants (Solano et al. 1998; Yanagisawa et al. 2003). In this study, an EIN3 homologous gene (*VaEIN3.1*) was identified in the grapevine. Results from OE and knockdown materials supported the key roles of *VaEIN3.1* in delivering the signals from ethylene to downstream functional genes. Here, VaEIN3.1-VaERF05-VaFBA1 module provides new clues to explain how the ethylene signalling regulates the cold stress response process and contributes to the cold tolerance in plants (Figure 10). And the function of VaEIN3.1 in regulating the expression of other ethylene-induced genes during cold stress response in grapevines still needs to be studied in the future.

Acknowledgements

We acknowledge Prof. Chunying Kang of Huazhong Agricultural University for the provision of CRISPR-Cas9 vector.

Conflicts of Interest

The authors declare no conflicts of interest.

Data Availability Statement

Data will be made available on request.

References

Alonso, J. M., and A. N. Stepanova. 2004. "The Ethylene Signaling Pathway." *Science* 306, no. 5701: 1513–1515. https://doi.org/10.1126/science.1104812.

Amor, N. B., A. Jiménez, W. Megdiche, M. Lundqvist, F. Sevilla, and C. Abdelly. 2007. "Kinetics of the Anti-Oxidant Response to Salinity in the Halophyte *Cakile maritima*." *Journal of Integrative Plant Biology* 49, no. 7: 982–992. https://doi.org/10.1111/j.1672-9072.2007.00491.x.

Bartlett, A., R. C. O'Malley, S. C. Huang, et al. 2017. "Mapping Genome-Wide Transcription-Factor Binding Sites Using DAP-seq." *Nature Protocols* 12, no. 8: 1659–1672. https://doi.org/10.1038/nprot.2017.055.

Cai, B., Q. Li, F. Liu, H. Bi, and X. Ai. 2018. "Decreasing Fructose-1,6-Bisphosphate Aldolase Activity Reduces Plant Growth and Tolerance to Chilling Stress in Tomato Seedlings." *Physiologia Plantarum* 163, no. 2: 247–258. https://doi.org/10.1111/ppl.12682.

Chao, Q., M. Rothenberg, R. Solano, G. Roman, W. Terzaghi, and J. R. Ecker†. 1997. "Activation of the Ethylene Gas Response Pathway in *Arabidopsis* by the Nuclear Protein Ethylene-Insensitive3 and Related Proteins." *Cell* 89, no. 7: 1133–1144. https://doi.org/10.1016/S0092-8674(00)80300-1.

Chen, C., Y. Wu, J. Li, et al. 2023. "TBtools-II: A One for All, All for One' Bioinformatics Platform for Biological Big-Data Mining." *Molecular Plant* 16, no. 11: 1733–1742. https://doi.org/10.1016/j.molp.2023.09.010.

Chen, Y., Y. Dai, Y. Li, et al. 2022. "Overexpression of the *Salix matsudana* SmAP2-17 Gene Improves *Arabidopsis* Salinity Tolerance by Enhancing the Expression of SOS3 and ABI5." *BMC Plant Biology* 22, no. 1: 102. https://doi.org/10.1186/s12870-022-03487-y.

Contento, A. L., S. J. Kim, and D. C. Bassham. 2004. "Transcriptome Profiling of the Response of *Arabidopsis* Suspension Culture Cells to Suc Starvation." *Plant Physiology* 135, no. 4: 2330–2347. https://doi.org/10.1104/pp.104.044362.

Couée, I., C. Sulmon, G. Gouesbet, and A. El Amrani. 2006. "Involvement of Soluble Sugars in Reactive Oxygen Species Balance and Responses to Oxidative Stress in Plants." *Journal of Experimental Botany* 57, no. 3: 449–459. https://doi.org/10.1093/jxb/erj027.

Dahro, B., F. Wang, T. Peng, and J. H. Liu. 2016. "PtrA/NINV, an Alkaline/Neutral Invertase Gene of *Poncirus trifoliata*, Confers Enhanced Tolerance to Multiple Abiotic Stresses by Modulating ROS Levels and Maintaining Photosynthetic Efficiency." *BMC Plant Biology* 16: 76. https://doi.org/10.1186/s12870-016-0761-0.

Dubouzet, J. G., Y. Sakuma, Y. Ito, et al. 2003. "OsDREB Genes in Rice, *Oryza sativa* L., Encode Transcription Activators That Function in Drought-, High-Salt- and Cold-Responsive Gene Expression." *Plant Journal* 33, no. 4: 751–763. https://doi.org/10.1046/j.1365-313X.2003.01661.x.

Fennell, A. 2004. "Freezing Tolerance and Injury in Grapevines." *Journal of Crop Improvement* 10, no. 1–2: 201–235. https://doi.org/10.1300/J411v10n01_09.

Fu, J., Y. Zhao, Y. Zhou, et al. 2024. "MrERF039 Transcription Factor Plays an Active Role in the Cold Response of *Medicago ruthenica* as a Sugar Molecular Switch." *Plant, Cell & Environment* 47, no. 5: 1834–1851. https://doi.org/10.1111/pce.14845.

Geng, J., and J. H. Liu. 2018. "The Transcription Factor CsbHLH18 of Sweet Orange Functions in Modulation of Cold Tolerance and Homeostasis of Reactive Oxygen Species by Regulating the Antioxidant Gene." *Journal of Experimental Botany* 69, no. 10: 2677–2692. https://doi.org/10.1093/jxb/ery065.

Han, Q., J. Qi, G. Hao, et al. 2020. "ZmDREB1A Regulates Raffinose Synthase Controlling Raffinose Accumulation and Plant Chilling Stress Tolerance in Maize." *Plant & Cell Physiology* 61, no. 2: 331–341. https://doi.org/10.1093/pcp/pcz200.

He, Y., W. Zhang, X. Zuo, et al. 2024. "Dynamic Transcriptomics Unveils Parallel Transcriptional Regulation in Artemisinin and Phenylpropanoid Biosynthesis Pathways Under Cold Stress in *Artemisia annua*." *Scientific Reports* 14, no. 1: 31213. https://doi.org/10.1038/s41598-024-82551-z.

Hou, Y., D. C. J. Wong, Q. Li, et al. 2023. "Dissecting the Effect of Ethylene in the Transcriptional Regulation of Chilling Treatment in Grapevine Leaves." *Plant Physiology and Biochemistry* 196: 1084–1097. https://doi.org/10.1016/j.plaphy.2023.03.015.

Hou, Y., D. C. J. Wong, X. Sun, et al. 2024. "*VvbHLH036*, a Basic Helix-Loop-Helix Transcription Factor Regulates the Cold Tolerance of Grapevine." *Plant Physiology* 196, no. 4: 2871–2889. https://doi.org/10.1093/plphys/kiae483.

Hu, C., M. Wang, C. Zhu, et al. 2024. "A Transcriptional Regulation of ERF15 Contributes to ABA-Mediated Cold Tolerance in Tomato." *Plant, Cell & Environment* 47, no. 4: 1334–1347. https://doi.org/10.1111/pce.14816.

Huang, J., X. Zhao, M. Bürger, J. Chory, and X. Wang. 2023. "The Role of Ethylene in Plant Temperature Stress Response." *Trends in Plant Science* 28, no. 7: 808–824. https://doi.org/10.1016/j.tplants.2023.03.001.

Khan, M., B. Dahro, Y. Wang, et al. 2024. "The Transcription Factor ERF110 Promotes Cold Tolerance by Directly Regulating Sugar and Sterol Biosynthesis in Citrus." *Plant Journal* 119: 2385–2401. https://doi.org/10.1111/tpj.16925.

Khan, M., J. Hu, B. Dahro, et al. 2021. "ERF108 From *Poncirus trifoliata* (L.) Raf. Functions in Cold Tolerance by Modulating Raffinose Synthesis Through Transcriptional Regulation of *PtrRafS*." *Plant Journal* 108, no. 3: 705–724. https://doi.org/10.1111/tpj.15465.

Kong, L., Q. Song, H. Wei, et al. 2023. "The AP2/ERF Transcription Factor PtoERF15 Confers Drought Tolerance via JA-Mediated Signaling in *Populus*." *New Phytologist* 240, no. 5: 1848–1867. https://doi.org/10.1111/nph.19251.

Kumar, K. R. R., and P. B. Kirti. 2010. "A Mitogen-Activated Protein Kinase, AhMPK6 From Peanut Localizes to the Nucleus and Also Induces Defense Responses Upon Transient Expression in Tobacco." *Plant Physiology and Biochemistry* 48: 481–486. https://doi.org/10.1016/j.plaphy.2010.03.010.

Li, C., J. Su, N. Zhao, et al. 2023. "CmERF5-CmRAP2.3 Transcriptional Cascade Positively Regulates Waterlogging Tolerance in *Chrysanthemum morifolium*." *Plant Biotechnology Journal* 21, no. 2: 270–282. https://doi.org/10.1111/pbi.13940.

Li, Q., H. Zhou, F. Chai, et al. 2025. "Identification of Potential Metabolites Responsible for Cold Tolerance in Buds of *Vitis amurensis*." *Horticultural Plant Journal* 11, no. 1: 175–188. https://doi.org/10.1016/j.hpj.2023.07.009.

Liang, G., H. Wang, H. Gou, et al. 2024. "Overexpression of VaBAM3 From *Vitis amurensis* Enhances Seedling Cold Tolerance by Promoting Soluble Sugar Accumulation and Reactive Oxygen Scavenging." *Plant Cell Reports* 43, no. 6: 151. https://doi.org/10.1007/s00299-024-03236-5.

Liu, Q., C. Wang, X. Jiao, et al. 2019. "Hi-TOM: A Platform for High-Throughput Tracking of Mutations Induced by CRISPR/Cas Systems." *Science China Life Sciences* 62, no. 1: 1–7. https://doi.org/10.1007/s11427-018-9402-9.

Liu, S., Y. Zheng, L. Zhao, M. Gulam, A. Ullah, and G. Xie. 2024. "Calmodulin-Like16 and Pin-Likes7a Cooperatively Regulate Rice Seedling Primary Root Elongation under Chilling." *Plant Physiology* 195: 1660–1680. https://doi.org/10.1093/plphys/kiae130.

Lu, W., X. Tang, Y. Huo, et al. 2012. "Identification and Characterization of Fructose 1,6-Bisphosphate Aldolase Genes in Arabidopsis Reveal a Gene Family With Diverse Responses to Abiotic Stresses." *Gene* 503, no. 1: 65–74. https://doi.org/10.1016/j.gene.2012.04.042.

Lv, K., J. Li, K. Zhao, et al. 2020. "Overexpression of an AP2/ERF Family Gene, BpERF13, in Birch Enhances Cold Tolerance Through Upregulating CBF Genes and Mitigating Reactive Oxygen Species." *Plant Science* 292: 110375. https://doi.org/10.1016/j.plantsci.2019.110375.

Machanick, P., and T. L. Bailey. 2011. "MEME-ChIP: Motif Analysis of Large DNA Datasets." *Bioinformatics* 27, no. 12: 1696–1697. https://doi.org/10.1093/bioinformatics/btr189.

Magnan, F., B. Ranty, M. Charpenteau, B. Sotta, J. P. Galaud, and D. Aldon. 2008. "Mutations in AtCML9, a Calmodulin-Like Protein From *Arabidopsis thaliana*, Alter Plant Responses to Abiotic Stress and Abscisic Acid." *Plant Journal* 56, no. 4: 575–589. https://doi.org/10.1111/j.1365-313X.2008.03622.x.

Meng, X., S. Liu, T. Dong, et al. 2020. "Identification, Expression Analysis, and Functional Characterization of Salt Stress-Responsive Genes of AP2/ERF Transcription Factors in Sweet Potato." *Crop Science* 60, no. 6: 3247–3260. https://doi.org/10.1002/csc2.20290.

Mu, J., Y. Fu, B. Liu, et al. 2021. "*SiFBA5*, a Cold-Responsive Factor From *Saussurea involucrata* Promotes Cold Resilience and Biomass Increase in Transgenic Tomato Plants Under Cold Stress." *BMC Plant Biology* 21, no. 1: 75. https://doi.org/10.1186/s12870-021-02851-8.

Mu, H., Y. Li, L. Yuan, et al. 2023. "MYB30 and MYB14 Form a Repressor-Activator Module With WRKY8 That Controls Stilbene Biosynthesis in Grapevine." *Plant Cell* 35, no. 1: 552–573. https://doi.org/10.1093/plcell/koac308.

Munir, S., H. Liu, Y. Xing, et al. 2016. "Overexpression of Calmodulin-Like (*ShCML44*) Stress-Responsive Gene From *Solanum habrochaites* Enhances Tolerance to Multiple Abiotic Stresses." *Scientific Reports* 6: 31772. https://doi.org/10.1038/srep31772.

Nakabayashi, R., and K. Saito. 2015. "Integrated Metabolomics for Abiotic Stress Responses in Plants." *Current Opinion in Plant Biology* 24: 10–16. https://doi.org/10.1016/j.pbi.2015.01.003.

O'Hara, L. E., M. J. Paul, and A. Wingler. 2013. "How Do Sugars Regulate Plant Growth and Development? New Insight Into the Role of Trehalose-6-Phosphate." *Molecular Plant* 6, no. 2: 261–274. https://doi.org/10.1093/mp/sss120.

Ohme-Takagi, M., and H. Shinshi. 1995. "Ethylene-Inducible DNA Binding Proteins That Interact With an Ethylene-Responsive Element." *Plant Cell* 7: 173–182. https://doi.org/10.1105/tpc.7.2.173.

Park, H. C., C. Y. Park, S. C. Koo, et al. 2010. "AtCML8, a Calmodulin-Like Protein, Differentially Activating CaM-Dependent Enzymes in *Arabidopsis thaliana*." *Plant Cell Reports* 29, no. 11: 1297–1304. https://doi.org/10.1007/s00299-010-0916-7.

Peng, K., Y. Tian, J. Cang, et al. 2022. "Overexpression of *TaFBA-A10* From Winter Wheat Enhances Freezing Tolerance in *Arabidopsis thaliana*." *Journal of Plant Growth Regulation* 41, no. 1: 314–326. https://doi.org/10.1007/s00344-021-10304-7.

Peng, T., X. Zhu, N. Duan, and J. H. Liu. 2014. "PtrBAM1, a β-Amylase-Coding Gene of *Poncirus trifoliata*, Is a CBF Regulon Member With Function in Cold Tolerance by Modulating Soluble Sugar Levels." *Plant, Cell & Environment* 37, no. 12: 2754–2767. https://doi.org/10.1111/pce.12384.

Plaxton, W. C. 1996. "The Organization and Regulation of Plant Glycolysis." *Annual Review of Plant Physiology and Plant Molecular Biology* 47, no. 1: 185–214. https://doi.org/10.1146/annurev.arplant.47.1.185.

Ren, C., P. Fan, S. Li, and Z. Liang. 2023. "Advances in Understanding Cold Tolerance in Grapevine." *Plant Physiology* 192, no. 3: 1733–1746. https://doi.org/10.1093/plphys/kiad092.

Rutter, W. J. 1964. "Evolution of Aldolase." *Federation Proceedings* 23: 1248–1257.

Sakuma, Y., Q. Liu, J. G. Dubouzet, H. Abe, K. Shinozaki, and K. Yamaguchi-Shinozaki. 2002. "DNA-Binding Specificity of the ERF/AP2 Domain of Arabidopsis DREBs, Transcription Factors Involved in Dehydration- and Cold-Inducible Gene Expression." *Biochemical and Biophysical Research Communications* 290, no. 3: 998–1009. https://doi.org/10.1006/bbrc.2001.6299.

Shi, Y., S. Tian, L. Hou, et al. 2012. "Ethylene Signaling Negatively Regulates Freezing Tolerance by Repressing Expression of CBF and Type-A ARR Genes in *Arabidopsis*." *Plant Cell* 24: 2578–2595. https://doi.org/10.1105/tpc.112.098640.

Solano, R., A. Stepanova, Q. Chao, and J. R. Ecker. 1998. "Nuclear Events in Ethylene Signaling: A Transcriptional Cascade Mediated by Ethylene-Insensitive3 and Ethylene-Response-Factor1." *Genes & Development* 12, no. 23: 3703–3714. https://doi.org/10.1101/gad.12.23.3703.

Sperdouli, I., and M. Moustakas. 2012. "Interaction of Proline, Sugars, and Anthocyanins During Photosynthetic Acclimation of *Arabidopsis thaliana* to Drought Stress." *Journal of Plant Physiology* 169, no. 6: 577–585. https://doi.org/10.1016/j.jplph.2011.12.015.

Sun, Q., R. Huang, H. Zhu, Y. Sun, and Z. Guo. 2021. "A Novel *Medicago Truncatula* Calmodulin-Like Protein (MtCML42) Regulates Cold Tolerance and Flowering Time." *Plant Journal* 108, no. 4: 1069–1082. https://doi.org/10.1111/tpj.15494.

Sun, X., L. Zhang, D. C. J. Wong, et al. 2019. "The Ethylene Response Factor *VaERF092* From Amur Grape Regulates the Transcription Factor VaWRKY33, Improving Cold Tolerance." *Plant Journal* 99, no. 5: 988–1002. https://doi.org/10.1111/tpj.14378.

Sun, X., T. Zhao, S. Gan, et al. 2016. "Ethylene Positively Regulates Cold Tolerance in Grapevine by Modulating the Expression of Ethylene Response Factor 057." *Scientific Reports* 6: 24066. https://doi.org/10.1038/srep24066.

Tamura, K., G. Stecher, and S. Kumar. 2021. "MEGA11: Molecular Evolutionary Genetics Analysis Version 11." *Molecular Biology and Evolution* 38, no. 7: 3022–3027. https://doi.org/10.1093/molbev/msab120.

Wang, B., C. Wu, G. Wang, J. He, and S. Zhu. 2021. "Transcriptomic Analysis Reveals a Role of Phenylpropanoid Pathway in the Enhancement of Chilling Tolerance by Pre-Storage Cold Acclimation in Cucumber Fruit." *Scientia Horticulturae* 288: 110282. https://doi.org/10.1016/j.scienta.2021.110282.

Wang, M., W. Dai, J. Du, R. Ming, B. Dahro, and J. H. Liu. 2019. "*ERF109* of Trifoliate Orange (*Poncirus trifoliata* (L.) Raf.) Contributes to Cold Tolerance by Directly Regulating Expression of *Prx1* Involved in Antioxidative Process." *Plant Biotechnology Journal* 17, no. 7: 1316–1332. https://doi.org/10.1111/pbi.13056.

Wang, Y., H. Jiang, Z. Mao, et al. 2021. "Ethylene Increases the Cold Tolerance of Apple via the MdERF1B–MdCIbHLH1 Regulatory Module." *Plant Journal* 106, no. 2: 379–393. https://doi.org/10.1111/tpj.15170.

Wu, Y., X. Li, J. Zhang, et al. 2022. "ERF Subfamily Transcription Factors and Their Function in Plant Responses to Abiotic Stresses." *Frontiers in Plant Science* 13: 1042084. https://doi.org/10.3389/fpls.2022.1042084.

Xie, Z., T. Nolan, H. Jiang, et al. 2019. "The AP2/ERF Transcription Factor Tiny Modulates Brassinosteroid-Regulated Plant Growth and Drought Responses in *Arabidopsis*." *Plant Cell* 31, no. 8: 1788–1806. https://doi.org/10.1105/tpc.18.00918.

Xin, H., W. Zhu, L. Wang, et al. 2013. "Genome Wide Transcriptional Profile Analysis of *Vitis amurensis* and *Vitis vinifera* in Response to Cold Stress." *PLoS One* 8: e58740. https://doi.org/10.1371/journal.pone.0058740.

Xu, G. Y., P. S. C. F. Rocha, M. L. Wang, et al. 2011. "A Novel Rice Calmodulin-Like Gene, *OsMSR2*, Enhances Drought and Salt Tolerance and Increases ABA Sensitivity in Arabidopsis." *Planta* 234, no. 1: 47–59. https://doi.org/10.1007/s00425-011-1386-z.

Xu, L., L. Yang, A. Li, et al. 2024. "An AP2/ERF Transcription Factor Confers Chilling Tolerance in Rice." *Science Advances* 10, no. 35: 1–16. https://doi.org/10.1126/sciadv.ado4788.

Yamaguchi, T., G. S. Aharon, J. B. Sottosanto, and E. Blumwald. 2005. "Vacuolar Na^+/H^+ Antiporter Cation Selectivity Is Regulated by Calmodulin From Within the Vacuole in a Ca^{2+}- and pH-Dependent Manner." *Proceedings of the National Academy of Sciences* 102: 16107–16112. https://doi.org/10.1073/pnas.0504437102.

Yamaguchi-Shinozaki, K., and K. Shinozaki. 1994. "A Novel Cis-Acting Element in an *Arabidopsis* Gene Is Involved in Responsiveness to Drought, Low-Temperature, or High-Salt Stress." *Plant Cell* 6, no. 2: 251–264. https://doi.org/10.2307/3869643.

Yanagisawa, S., S. D. Yoo, and J. Sheen. 2003. "Differential Regulation of EIN3 Stability by Glucose and Ethylene Signalling in Plants." *Nature* 425, no. 6957: 521–525. https://doi.org/10.1038/nature01984.

Yao, Y., R. J. He, Q. L. Xie, et al. 2017. "Ethylene Response Factor 74 (ERF74) Plays an Essential Role in Controlling a Respiratory Burst Oxidase Homolog D (RbohD)-Dependent Mechanism in Response to Different Stresses in Arabidopsis." *New Phytologist* 213, no. 4: 1667–1681. https://doi.org/10.1111/nph.14278.

Yu, G., L. G. Wang, and Q. Y. He. 2015. "ChIPseeker: An R/Bioconductor Package for Chip Peak Annotation, Comparison and Visualization." *Bioinformatics* 31, no. 14: 2382–2383. https://doi.org/10.1093/bioinformatics/btv145.

Yu, S., J. Wu, Y. Sun, et al. 2022. "A Calmodulin-Like Protein (CML10) Interacts With Cytosolic Enzymes GSTU8 and FBA6 to Regulate Cold Tolerance." *Plant Physiology* 190, no. 2: 1321–1333. https://doi.org/10.1093/plphys/kiac311.

Zhang, M., M. Zhang, J. Wang, et al. 2023. "Salicylic Acid Regulates Two Photosystem II Protection Pathways in Tomato Under Chilling Stress Mediated by Ethylene Insensitive 3-Like Proteins." *Plant Journal* 114, no. 6: 1385–1404. https://doi.org/10.1111/tpj.16199.

Zhang, Y., T. Liu, C. A. Meyer, et al. 2008. "Model-Based Analysis of ChIP-Seq (MACS)." *Genome Biology* 9, no. 9: R137. https://doi.org/10.1186/gb-2008-9-9-r137.

Zhang, Y., R. Ming, M. Khan, et al. 2022. "ERF9 of *Poncirus trifoliata* (L.) Raf. Undergoes Feedback Regulation by Ethylene and Modulates Cold Tolerance via Regulating a Glutathione S-Transferase U17 Gene." *Plant Biotechnology Journal* 20, no. 1: 183–200. https://doi.org/10.1111/pbi.13705.

Zhao, H., C. C. Yin, B. Ma, S. Y. Chen, and J. S. Zhang. 2021. "Ethylene Signaling in Rice and *Arabidopsis*: New Regulators and Mechanisms." *Journal of Integrative Plant Biology* 63, no. 1: 102–125. https://doi.org/10.1111/jipb.13028.

Zhou, H., Q. Li, D. K. Gichuki, et al. 2023. "Dynamics of Starch Degradation and Expression of Related Genes During Chilling Stress in Grapevine." *Horticulture Advances* 1: 3. https://doi.org/10.1007/s44281-023-00004-5.

Zhuo, C., L. Liang, Y. Zhao, Z. Guo, and S. Lu. 2018. "A Cold Responsive Ethylene Responsive Factor From *Medicago falcata* Confers Cold Tolerance by Up-Regulation of Polyamine Turnover, Antioxidant Protection, and Proline Accumulation." *Plant, Cell & Environment* 41, no. 9: 2021–2032. https://doi.org/10.1111/pce.13114.

Supporting Information

Additional supporting information can be found online in the Supporting Information section.